AD-A154 168 PRODUCTION VERIFICATION OF THE ACOUSTIC EMISSION WELD MONITOR(U) CHAMBERLAIN NATIONAL NILES IL GARD DIV I R KRASKA ET AL. MAY 84 TACOM-TR-12988 1/2

UNCLASSIFIED DAAE07-82-C-4116 F/G 11/6 NL

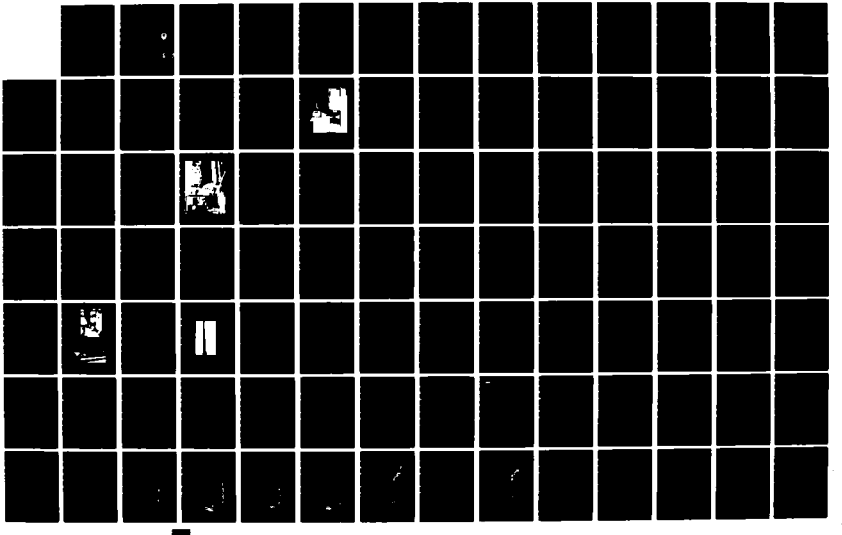

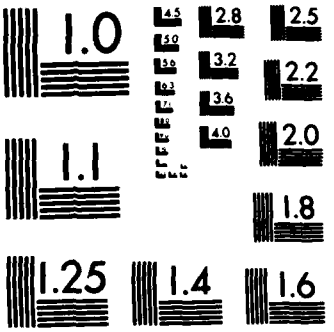

MICROCOPY RESOLUTION TEST CHART
NATIONAL BUREAU OF STANDARDS-1963-A

AD-A154 168

R and D TACOM

TECHNICAL REPORT

NO. 12988

PRODUCTION VERIFICATION OF THE ACOUSTIC EMISSION WELD MONITOR

Final Report

CONTRACT NO. DAAE07-82-C-4116

by Chamberlain Manufacturing Corporation
GARD Division
Niles, Illinois 60648

I. R. Kraska
W. L. Lichodziejewski
J. E. Condray

TACOM

R. Crow III

DTIC FILE COPY

DTIC ELECTE MAY 24 1985 S D A

Approved for Public Release: Distribution Unlimited

U.S. ARMY TANK-AUTOMOTIVE COMMAND
Warren, Michigan 48090

NOTICES

This report is not to be construed as an official Department of the Army position.

Mention of any trade names or manufacturers in this report shall not be construed as an official endorsement or approval of such products or companies by the U. S. Government.

Destroy this report when it is no longer needed. Do not return it to the originator.

SECURITY CLASSIFICATION OF THIS PAGE (When Data Entered)

REPORT DOCUMENTATION PAGE	READ INSTRUCTIONS BEFORE COMPLETING FORM
1. REPORT NUMBER: 12988 — 2. GOVT ACCESSION NO.: AD-A154 168	3. RECIPIENT'S CATALOG NUMBER
4. TITLE (and Subtitle): Production Verification of the Acoustic Emission Weld Monitor	5. TYPE OF REPORT & PERIOD COVERED: Final Report
	6. PERFORMING ORG. REPORT NUMBER: DAAE07-82-C-4116
7. AUTHOR(s): I. R. Kraska, J. Condray, W. L.Lichodziejewski, R. Crow III	8. CONTRACT OR GRANT NUMBER(s)
9. PERFORMING ORGANIZATION NAME AND ADDRESS: Chamberlain National - GARD Division, Niles, Illinois 60648	10. PROGRAM ELEMENT, PROJECT, TASK AREA & WORK UNIT NUMBERS
11. CONTROLLING OFFICE NAME AND ADDRESS: U. S. Army Tank-Automotive Command, Warren, Michigan 48090, Attn: R. Crow III/DRSTA-QAT	12. REPORT DATE: May 1984
	13. NUMBER OF PAGES: 99
14. MONITORING AGENCY NAME & ADDRESS(if different from Controlling Office)	15. SECURITY CLASS. (of this report): Unclassified
	15a. DECLASSIFICATION/DOWNGRADING SCHEDULE

16. DISTRIBUTION STATEMENT (of this Report)

For Public dissemination, distribution unlimited

17. DISTRIBUTION STATEMENT (of the abstract entered in Block 20, if different from Report)

18. SUPPLEMENTARY NOTES

19. KEY WORDS (Continue on reverse side if necessary and identify by block number)

Nondestructive testing,
Acoustic Emission,
Weld monitoring,
Weld inspection,
Armor plate welds,
Process control,

20. ABSTRACT (Continue on reverse side if necessary and identify by block number)

The reported work is Phase III of an Army program to develop a microprocessor-based Acoustic Emission Weld Monitor (AEWM) for the purpose of real-time monitoring of production armor plate welding.

The objective of this Phase was to determine how effectively the AEWM can detect, locate, and classify weld flaws in production and to establish credibility of acoustic emission (AE) as an effective production tool. To accomplish these objectives, GARD fabricated an AEWM designed to monitor armor-

DD FORM 1 JAN 73 1473 EDITION OF 1 NOV 65 IS OBSOLETE

SECURITY CLASSIFICATION OF THIS PAGE (When Data Entered)

plate, and performed a six-month extended field test to provide a large data base for analysis.

Twenty-five M1 tank hulls were evaluated with the AEWM and standard NDE tests. The results of the 6-month production test showed that 93 percent of the AE indications were confirmed by standard NDE tests. The AE detection model used is 83 percent accurate in identifying repairable flaws. (This can be improved to 88 percent with some changes in software.) The AE characterization model was 100 percent accurate in identification of the most significant repairable flaw - a crack. The system has an average locational accuracy of better than one inch. Don't Keywords include: see 1473

In addition to production weld monitoring the AEWM was used on two special problems. Preliminary indications from a brief series of weld monitoring experiments performed in the Lima MM&T Weld Lab, and subsequent production line monitoring of M1 tank hull welds, show encouraging delayed crack/delayed crack precursor detection results. One turret ring weld repair was successfully monitored with the AEWM.

PREFACE

This report presents the results of an evaluation of the Acoustic Emission Weld Monitor (AEWM) on production welding of the M1 tank hulls. The results show that acoustic emission correctly detected 93 percent of indicated flaws, as confirmed by standard NDE inspections. The data shows AE indication correlation with repairs was 83 percent. This latter accuracy can be upgraded to 88 percent by software changes to the defect detection model which was used. The data also shows that the AEWM was 100 percent accurate in characterizing cracks - the most significant weld flaw, and, that the AEWM is capable of locating flaws to within an average of better than one inch.

A brief series of weld monitoring experiments performed in the Lima MM&T Weld Lab, and subsequently on the production line shows good results on delayed crack and delayed crack precursor detection. In a special application, it was shown on an actual turret repair, that the AEWM can determine when crack removal is complete during weld metal removal (air-arcing), and can detect weld defects during subsequent repair welding.

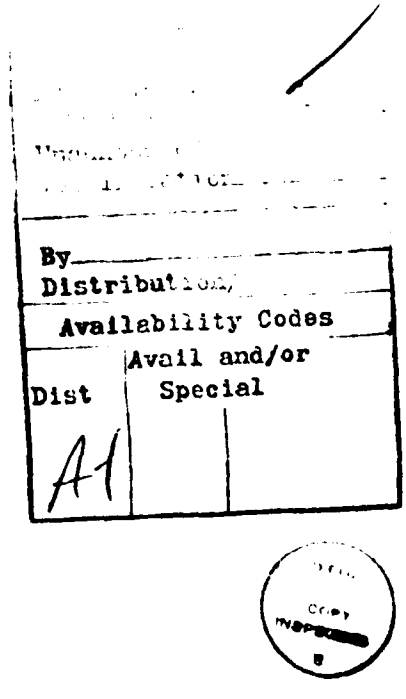

FOREWORD

The work described in this report was performed by Chamberlain National, GARD Division, 7501 N. Natchez Avenue, Niles, Illinois 60648 for the U.S. Army Tank-Automotive Command, under Contract No. DAAE07-82-C-4116. The work was administered under the direction of Army Project Engineer Robert Crow of TACOM, Warren, Michigan.

The work was performed in the contractor's Electronic Systems Group, W. Lichodziejewski, Manager, by I. R. Kraska, Project Engineer, J. Condray, Associate Engineer, and T. A. Mathieson, Research Engineer with the assistance of D. W. Prine, Staff Engineer.

The authors gratefully acknowledge the technical assistance provided by the Army Project Engineer and the efforts of F.E. Alloway, R. W. Kearns, L. N. Seay, and D. E. Bourdon of General Dynamics for their assistance in making the production NDE results available for GARD's use in this program. The authors also acknowledge the General Dynamics assistance provided by F. Ade, Chief Welding Engineer, in production interfacing, and J. Kennedy, Welding Engineer, and Mike Furlong and Dave Hollon, Welding Technicians, in the fabrication of the weld plates used in the delayed crack studies.

This report covers work conducted during the period of September, 1982 to April, 1984.

This project has been accomplished as part of the U. S. Army Manufacturing Testing Technology Program, which has for its objective the timely establishment of testing techniques, procedures or prototype equipment (in mechanical, chemical, or nondestructive testing) to insure efficient inspection methods for materiel/ material procured or main tained by DARCOM.

The use of trade names in this report does not constitute an official endorsement or approval of such commercial hardware or software. This report may not be cited for purposes of advertisement.

TABLE OF CONTENTS

THIS PAGE LEFT BLANK INTENTIONALLY

LIST OF ILLUSTRATIONS

THIS PAGE LEFT BLANK INTENTIONALLY

LIST OF TABLES

THIS PAGE LEFT BLANK INTENTIONALLY

1.0 OBJECTIVE

The primary objectives of this program were to determine how effectively the AEWM can detect, locate, and classify weld flaws in production, and to establish credibility of AE as an effective production monitoring tool. To carry out these objectives, the following tasks were performed:

- o A study of the data masking effects of grinding and chipping to see if it might be possible to eliminate missing an AE flaw indication because of simultaneous grinding and chipping.
- o Fabrication of an Acoustic Emission Weld Monitor designed to monitor armor plate welds.
- o A six-month extended field test to provide a large data base for analysis.

The first Task is covered in the Appendix of this report. The remaining tasks of fabrication and production monitoring are covered in Sections 4 and 5.

2.0 SUMMARY

An Acoustic Emission Weld Monitor (AEWM) was fabricated for use in armor plate weld monitoring. The assembled system was then used at the Lima Army Tank Plant (LATP) in Lima, Ohio for six (extended to ten months) months of production line weld monitoring.

Twenty-five M1 tank hull welds were evaluated with the AEWM and standard NDE tests. The resultant analysis showed that 93 percent (40/43 - with 3 undercalls) of the AE indications were confirmed by standard NDE tests.

"Thresholding" of AE indications, by characterization and sizing number, provides AE indications of flaws requiring repair. Thresholding with the detection model used, shows an 83 percent accuracy in AE identification of flaws which required repairs as defined by Government standards invoked for M1 fabrication (19/23 - 3 with undercalls). This accuracy can be improved to 88 percent (22/25 - with 0 undercalls) by a change in porosity detection software, and the assumption that the one missed transverse crack (TV) was a delayed crack (i.e., not monitored).

The AEWM uses a five-category flaw characterization model. The data shows the current five-flaw model is 100 percent accurate in characterization of the most significant flaw - crack. It is 100 percent accurate in calling rejectable porosity correctly. The Unclassified category indicates acceptable porosity 100 percent of the time. The model is 23 percent accurate in calling incomplete penetration correctly, and 25 percent accurate in calling lack of fusion correctly.

The AEWM also provides flaw location in inches from the #1 sensor. Data analysis shows the AEWM locates flaws to within an average of better than 1 inch.

In addition to production weld monitoring, the AEWM was used on two special application problems. Preliminary indications from a brief series of weld monitoring experiments performed in the LATP MM&T Weld Lab, and subsequent production line tests, showed encouraging delayed crack/delayed crack precursor detection results. Delayed cracks were detected, located, and characterized by the AEWM as long as 11 hours after welding. Large amounts of low energy, high rate AE were detected during weld and post-weld monitoring in the welds that produced delayed cracks. In post-weld analysis the high rate low level AE activity was isolated as coming from the location of the detected delayed cracks, both before and during the crack activity. Similar low energy, high rate precursive AE was in evidence during the post-weld monitoring on production welds that produced AE detected delayed cracks.

One turret ring weld repair was successfully monitored by the AEWM. This effort demonstrated that the AEWM can determine if a crack has been removed during air-arcing, and can detect weld defects during subsequent repair welding.

3.0 CONCLUSIONS AND RECOMMENDATIONS

The AEWM, with its unique signal processing techniques, has shown to be an effective flaw detector and locator when used to monitor acoustic emission during the production welding of M1 tank hulls. The system was also demonstrated to be capable of characterizing flaws into crack (the most significant flaw) and non-crack-related categories, and to provide indications of flaw severity for accept/repair decisions. The AEWM signal processing eliminates the large amounts of background clutter normally associated with traditional AE monitoring approaches. This method provides greater sensitivity to serious planar flaws than does radiography. It is easier to apply than ultrasonic testing, in that sensors are fixed in position and require no scanning.

Production implementation of in-process AE monitoring would have its greatest impact on the weld repair process. It allows a weld to be repaired in-process (on a pass-by-pass basis) rather than after completion. This approach should not only reduce cost of fabrication through reduction of repair cost, but also minimize the damaging effects of post-fabrication multi-pass weld repair.

The ability to detect delayed cracks, further enhances the AEWM applicability to production M1 needs. The AE detection of delayed crack and delayed crack precursive activity was, however, a limited effort. The need exists for follow-on production work to optimize the real-time/precursor/delayed crack model developed herein.

The low energy, high rate precursive AE detected during in-process AE monitoring can also be an invaluable tool in studying the causes of delayed cracking in welds and work in this area should also be pursued.

Another area where AE could have an immediate impact in reducing weld repair costs is in-process monitoring of thick section repairs (i.e., turret rings). It can indicate whether the old flaw has been removed during air-arcing, and can detect new weld defects during repair welding.

In addition to production line and weld repair monitoring, the AEWM can be an educational enhancement in welder training/certification as it can provide indications of flaw formation at the time of occurrence rather than requiring post-weld radiography delay. This results in reduced training/certification time and cost. It also, allows quick optimization of welding procedures in the laboratory.

Automation of the M1 fabrication process is a high priority item of concern to both the Army and General Dynamics. For it to be successfully implemented, real-time welding process control is needed. The AE monitoring technology demonstrated here is a natural cornerstone for such control. Used as a real-time feedback mechanism, in conjunction with welding inputs (such as arc voltage, current, speed, and contamination), it will allow real-time determination of which weld parameters are causing flaws, and need correction.

4.0 INTRODUCTION

Acoustic Emission (AE) weld monitoring, and its use in the armor plate welding process, has been investigated for several years by the U.S. Army Tank-Automotive Command (TACOM). This effort has resulted in a

determination that acoustic emission weld monitoring shows potential as a weld process monitoring tool for providing quality welds of armor plate. The project described here is the third phase of a three-phase program.

Work in Phase I, completed in October, 1979, and reported in TARADCOM Technical Report No. 12468, entitled "Acoustic Emission Weld Monitoring System", consisted of the generation of laboratory welds in armor plate with the controlled introduction of critical flaw types. Recorded acoustic emission was correlated with radiographic, ultrasonic, and metallographic test results. The analysis showed that AE reliably detected intentional flaws.

Phase II, completed in September, 1981, and reported in TACOM Technical Report No. 12609 entitled "Acoustic Emission Monitoring of Production Armor Plate Welds", was directed toward the evaluation of AE when applied to production welding of heavy armored vehicles. In preparation for this task, flaw discrimination criteria were established, based on the data resulting from the Phase I effort. These data were refined thru a limited metallographic analysis of some of the early laboratory welds to gain further insight to the nature of natural flaws generated. The flaw discrimination criteria was then implemented in software form and checked out using the AE data gathered in Phase I. The software was then installed in an available hardened breadboard which was used for monitoring actual production welds at the Lima Army Tank Plant.

At Lima, after a trial production test to permit familiarization of production procedures, determination of Monitor settings, and finding optimal monitoring methods for this application, a two week production test was performed. Eleven production welds were monitored. Nineteen significant radiographic indications were identified; acoustic emission detected fifteen of them. Several application concerns were identified: weld geometry, effects of grinding masking of AE detection, and double weld monitoring.

Based upon on the favorable Phase II results, Phase III started. It involved (a) fabricating an Acoustic Emission Weld Monitor designed to monitor armor plate welds as defined in Phases I and II, (b) performing a study of the data masking effects of grinding to see if it might be possible to eliminate the small probability of missing an AE flaw indication because of simultaneous grinding, and (c) a six-month extended field test to provide a larger data base for analysis. The results are presented in the report.

4.1 AEWM Description

Figure 4.1 shows the Acoustic Emission Weld Monitor designed and fabricated for armor plate weld monitoring. The Acoustic Emission Weld Monitor is contained in the large cabinet at the right in the figure. This system uses three Motorola M6800 microprocessors. It has the capability of acquiring multi-channel acoustic emission data and performing the necessary data analysis to allow real-time detection, location, and characterization of flaws in weldments during welding. The system was fabricated for this program with three analog input channels, and incorporates the flaw detection, location, and characterization model evolved in Phase II. The hardware/software configuration includes the following features:

- o flaw pass/location storage for up to 255 Monitor start/stops (i.e., weld passes)
- o flaw characterization storage for up to 64 flaws
- o programming for C/L/IP/P/U flaw characterization (see page 21 for definitions)
- o EPROM-based firmware modifiable with flaw characterization models for special applications
- o remote start/stop capability
- o hardware lock via keyed power switch
- o Three location calibration modes: (a) self-calibration via round-robin transducer pulsing, (b) controlled self-calibration via pulsing of operator selected transducers, (c) manual calibration via operator entry of transducer intervals
- o Three signal processing channels
- o Two channel linear location algorithm
- o One guard channel
- o NEMA-12 type industrial cabinet
- o self-contained printer which lists flaw occurrence, location, type and relative size for each weld pass after pass completion

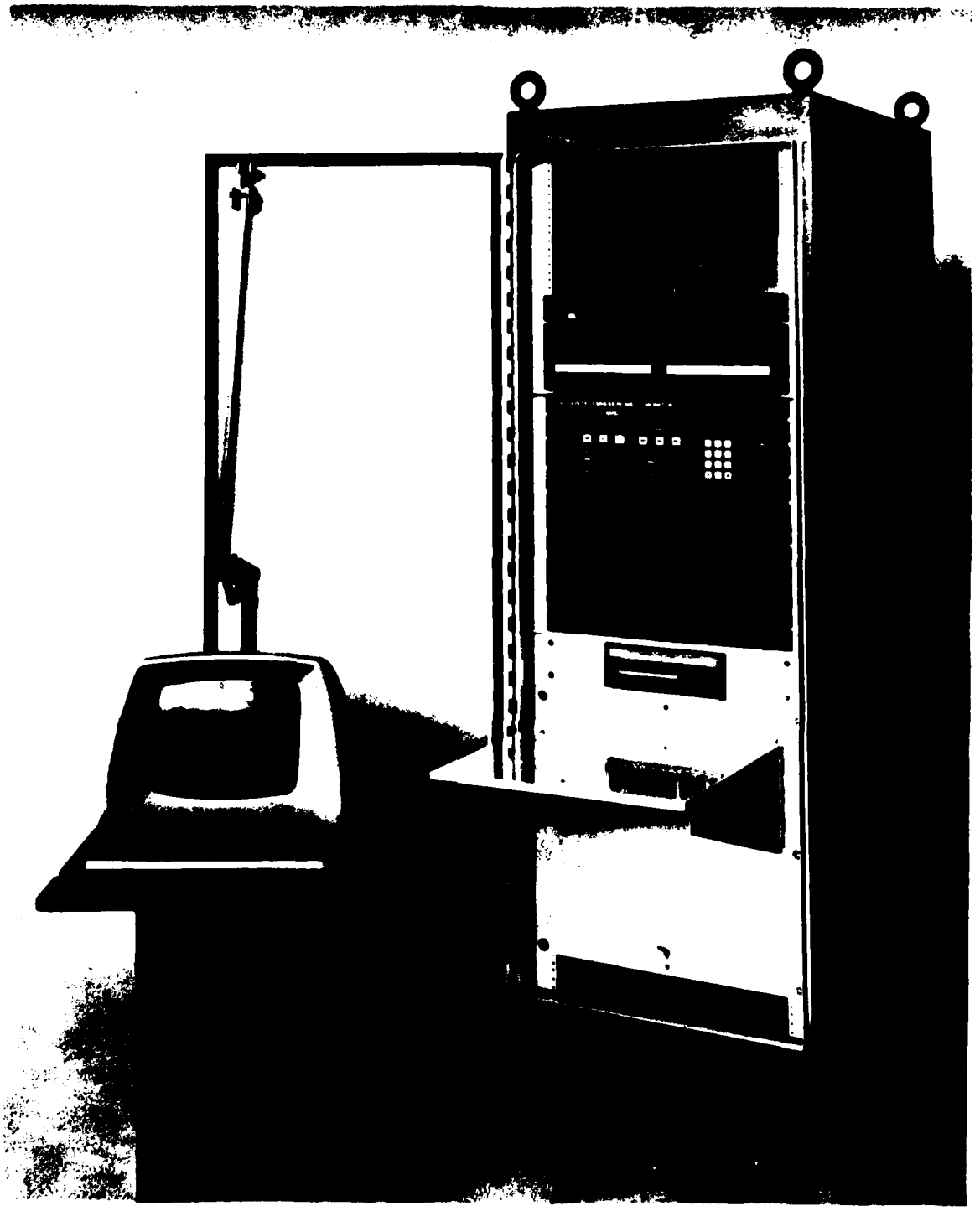

Figure 4.1 PRODUCTION AE WELD MONITOR

- o high temperature transducers (5)
- o magnetic hold-down assemblies (4)
- o transducer preamplifiers (5)
- o industrial-grade cables (6)

During initial production line weld monitoring a dual floppy disk system and a computer video terminal were used to augment the operation of the Weld Monitor. These pieces of equipment allow the recording of AE data on disk for post-weld analysis, and in addition, permit the operator to modify the processing parameters to allow optimization of Monitor performance for a particular set of weld conditions (i.e., material and process).

Details of System operation are provided in the AEWM Instruction Manual. Some general information is provided here as appropriate background to the Sections which follow later.

4.2 Guard Channel

As a result of a pre-production line monitoring visit to the Lima Army Tank Plant, it was determined that Hull Stations 1 and 2 were the most desirable for conducting the six-month production test. One unique aspect of the production situation is the simultaneous welding of the side to floor plate welds by two welders on the same hull. A 2-channel AEWM would not provide off-axis discrimination as to which weld was the source of the AE data. However, it was felt that with a 3-channel system and a 4-transducer array, extraneous AE data could be adequately isolated as to its source. Therefore, the AEWM was fabricated with a third "Guard" channel, with 2 transducer input, to isolate the extraneous AE data. Figure 4.2 is a schematic diagram which shows graphically how the "Guard band" accomplishes this task.

In the diagram, note the line (l_1- l_2) joining the midpoints between the channel 1 transducer and its associated channel 3 "Guard", and the channel 2 transducer and its associated channel 3 "Guard". By geometric considerations, sound originating above the line will arrive at one of the Guard transducers before reaching transducer 1 or transducer 2 (Reject Zone). Sound originating from any point below the line will arrive at transducer 1 or 2 before reaching either of the channel 3 transducers (Accept Zone).

As long as b > a, any AE originating from target weld will arrive at Ch 1 or Ch 2 before arriving at Ch 3.

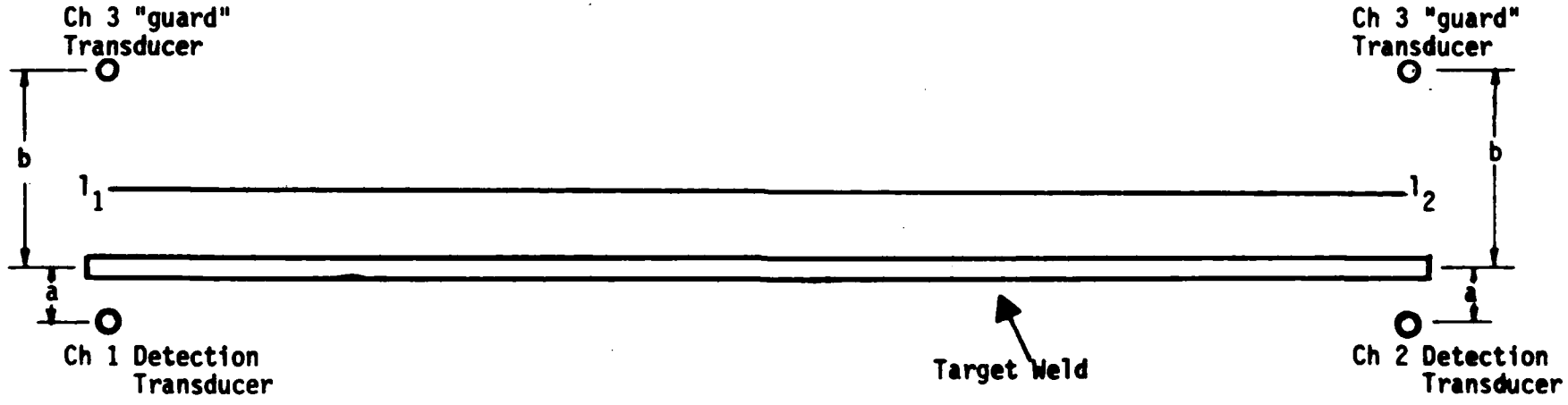

Figure 4.2 SCHEMATIC DIAGRAM OF GUARD BAND TRANSDUCER LAYOUT

The AEWM can record, on disk, each AE event and its related pre-processed data (including information on which transducer channel received the event first, second, and third). For flaw analysis/display it only uses events which did not reach the Guard transducers first (i.e., it rejects events from the Reject Zone). Two location "clock counts" exist in this AEWM: the first to count time between the first and second transducer channel "hit" times, the second to count time between the first and third "hit" times. From the weld of interest in the Accept Zone, the Guard transducers can be "hit" either second or third in the three transducer sequence. The AEWM automatically selects the correct clock count (representing the 1-2 tranducer interval) for event location calculation along the weld being monitored.

The flow chart in Figure 4.3 shows the procedure by which the AEWM processes acoustic emission signals for the Guard channel. This algorithm is based upon considerations of practicality, and has been well proven in practice. Theoretically if two events occur at both weld heads at the same time (within window sampling time) potential algorithm confusion could occur. Such a random occurrence would have to happen within a 1.6 msec time window. Since we only get about 1 event per second (600 events in 15 minutes), on the average we might expect this to happen once per 600 flaws (i.e., 1.6 msec/1000 msec). Therefore such an occurrence will cause small error and was ignored in algorithm implementation.

Another low probability theoretical condition leading to potential algorithm confusion would be an AE signal coming from a source exactly on the center line between the two welds of interest. Since there is no welding in this area, such an occurrence is highly unlikely and was ignored in algorithm implementation.

4.3 Signal Processing

The Flow Chart in Figure 4.4 shows the procedure by which the AEWM processes acoustic emission signals for flaw detection. The AE signals are subjected to three successive tests: energy or ringdown count limits, rate limits (AE bursts), and location tolerance. The parameter c is the number of energy-qualifying events required to initiate the flaw detector's rate test. The parameter t is the time in seconds into which all c events must fall for flaw detection. The limits r_l-r_h are, respectively, the lower and upper ringdown counts that create the energy qualification window. The number i is the algorithm described in Figure 4.3. The number j specifies which frequency band (described later in this section) is used in the flaw characterization process; the k defines the normalization frequency band, which is usually selected to

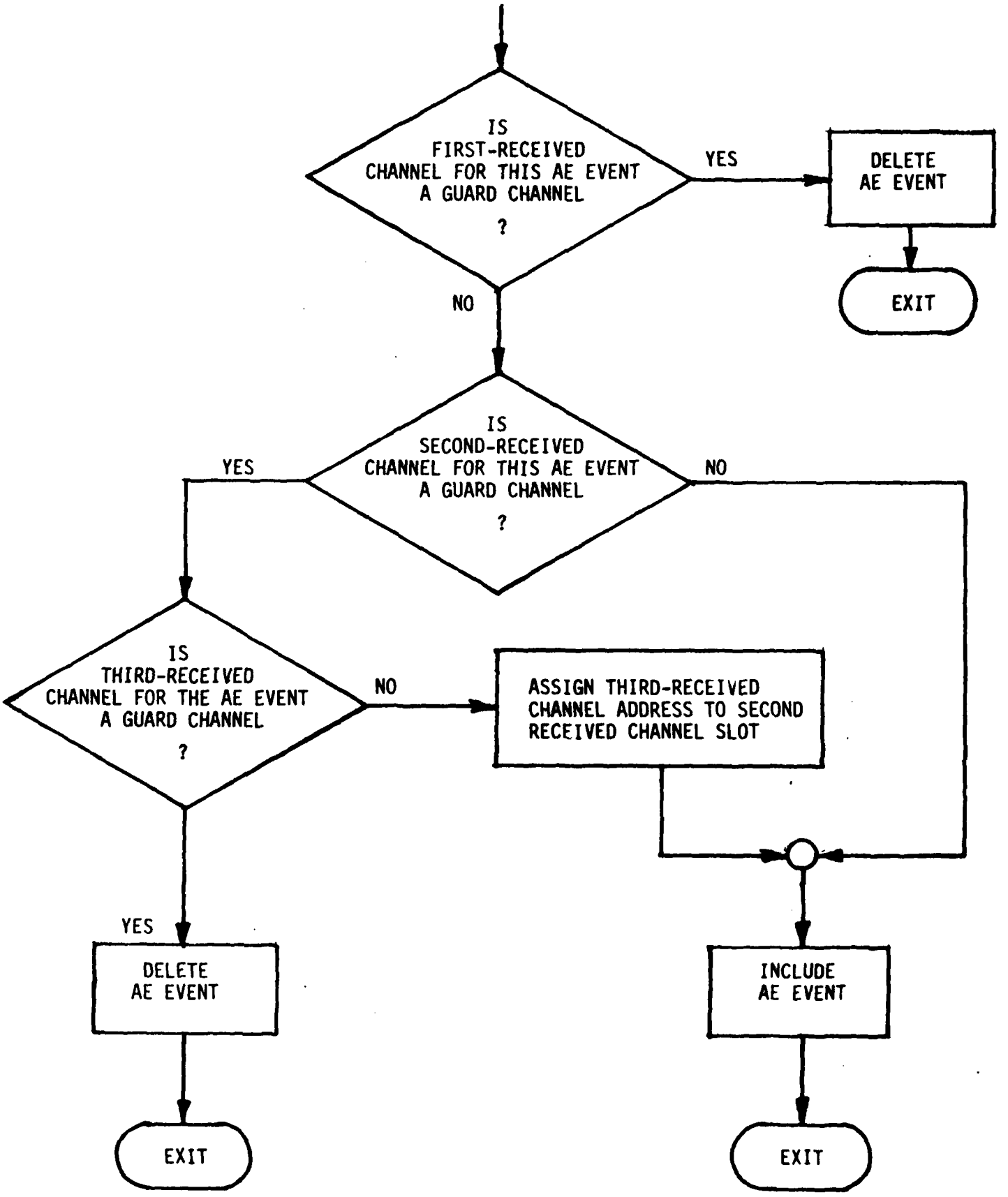

Figure 4.3 GUARD CHANNEL LOGIC

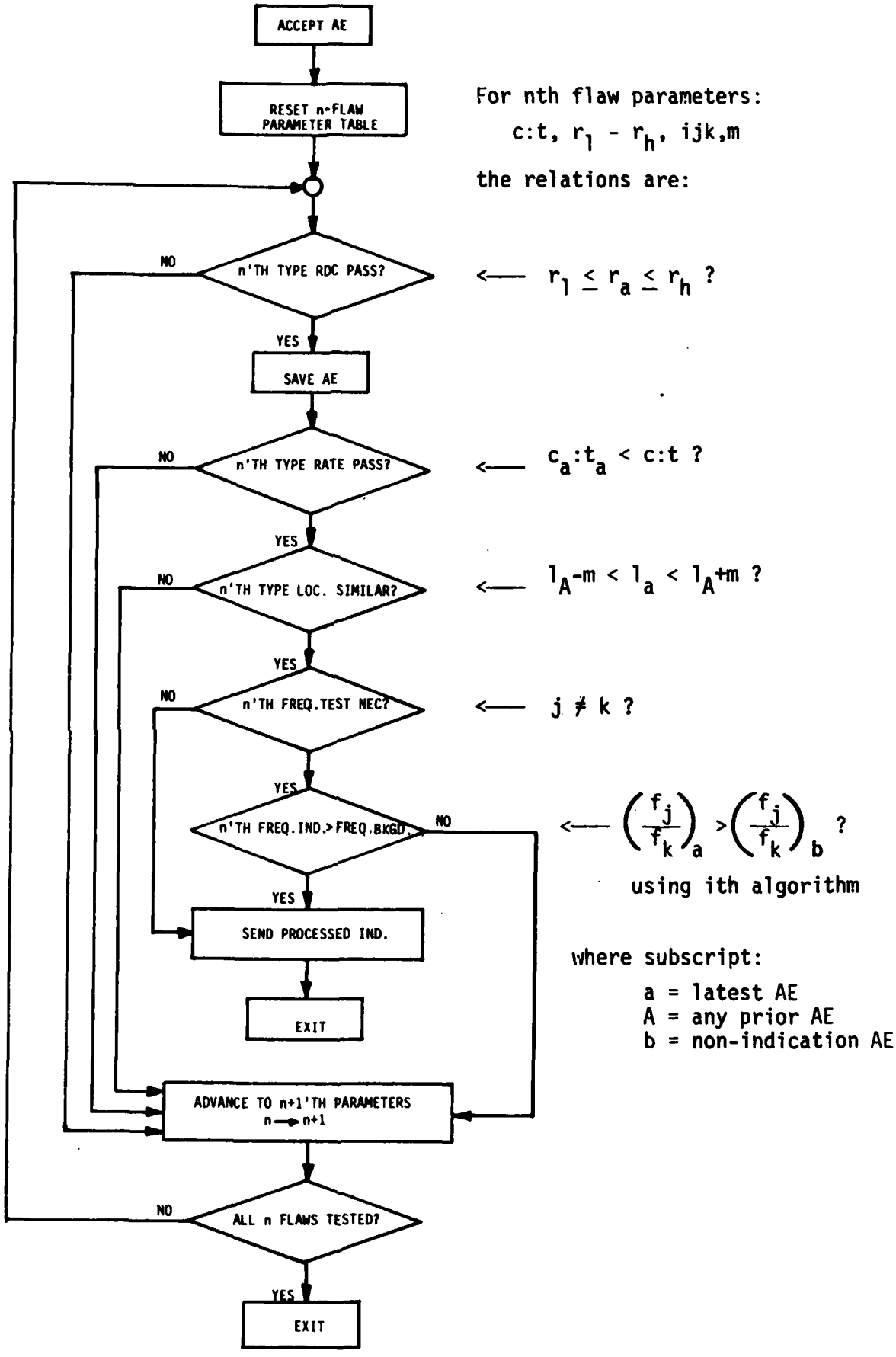

Figure 4.4 GENERALIZED DISCRIMINATION ALGORITHM

be the peak AE transducer response. The last number, m, is the locational tolerance used, it assures that all events being considered for a flaw indication must be from the same location $\pm$ the specified tolerance.

The effect of the ringdown count limits is to reject AE bursts which are either too low or too high in energy. The former result from continuous sources such as arc noise and electronic noise, while the latter generally are due to other non-flaw related processes such as weld clean-up (chipping and grinding). The rate and location criteria are based on the fact that a flaw generally produces higher rate AE than other sources, and the flaw-related events will all come from one localized point rather than be scattered over the weld length. The flaw detection model is a very powerful pattern recognition process and it is the essential link to success in application of AE to the high noise welding environment.

In addition to the detection test, all AE events have relative frequency spectral measurements made on them. These measurements are accomplished by using an eight channel comb filter that divides the frequency band from 100 kHz to 1 MHz into eight roughly equal bands (110, 150, 200, 270, 370,500, 675, and 920 kHz). These bands are numbered from 1 to 8, and identified as j and k in Figure 4.3.

The results of ratioing these spectral measurements are used to characterize the flaw-related acoustic emission as: "C", crack; "P", porosity; "L" lack of fusion; "I", incomplete penetration; and "U", unclassified. (This algorithm was developed and implemented in the Phase II production line test at Lima.) The following sections present specifics of the AE data processing procedure.

4.3.1 Flaw Detection

The flaw detection model found to be optimal for this work is quite similar to the model GARD has found to be optimum for a wide range of welding processes and materials. The detected acoustic emission events are subjected to three tests as shown in Figure 4.4. The parameters that proved optimum, based upon Phase II work are:

- Ringdown count limit: 96-1008
- Rate test: three or more events per second
- Locational tolerance: +/- 3 inches
- System gain: 60db using AET 175L sensors.

4.3.2 Flaw Characterization

The AEWM characterizes the flaw into five categories: crack, incomplete penetration, lack of fusion, porosity, and unclassified. During Phase II of the program a statistical analysis of AE data characteristics with radiographically-confirmed flaws augumented by metallographic data was performed to spot trends associated with specific flaw types. The results of this analysis was the flaw discrimination matrix shown in Table 4.1. Cracks, incomplete penetration, and lack of fusion are characterized as localized flaw types, with porosity tending towards a longer distribution of indications. In addition, porosity is characterized by a higher rate of emission with no specific frequency signature. Cracks, incomplete penetration, and lack of fusion are frequency-characterized; cracks and incomplete penetration are resolved by the consideration of pass number. By definition an incomplete penetration flaw is usually associated with a root pass, whereas the lack of fusion is associated with a high level pass. Thus, with pass information, characterization between incomplete penetration and lack of fusion is possible. Since detection is statistical, it is obvious that a category for AE which has the detection characteristics of the non-porosities but no specific frequency characteristic can exist. This is identified in the table as "unclassified'.

4.3.3 Flaw Sizing

The AEWM provides intensity data to correlate with flaw severity. The intensity number is the average ringdown count for the group of AE events that satisfy the flaw detection criteria (typically 3 or 4 events). The displayed severity number is a number ranging from 0 to 9 for ringdown counts ranging from 0 to 999 respectively.

4.4 Hard Copy Display

The System supports a built-in printer to provide permanent hard copy of the AE results. Figure 4.5 shows an example of printer readout giving all the pertinent test identifying parameters, as well as flaw locations, in both graphic and digital representation.

The AEWM status is continually displayed through the printer. Display and weld pass number are given in the printout. The printout also provides a header to identify (manually) test identifying parameters such as: hull number, date of inspection, gain setting, weld position and AEWM operator remarks.

The printing mode presents a listing of the active models for "C" crack, "I" incomplete penetration, "L" lack of fusion, "P" porosity, and "U" unclassified, respectively. For example, the program listing for "C" (crack) 3:1, 96-1008, 242, 0 would set the indication detector criteria to trip on sensing 3 events, within 1 second, having ringdown counts between 96 and 1008; the family 2 model is selected using the fourth band (220 kHz) normalized to the second band (150 kHz) for flaw characterization, with all three events required to come from the same location $\pm$ 1 inch.

The weld length is mapped by an array of thirty-two cells. The leftmost square in the display represents the position of the sensor connected to analog module 1 and the rightmost square represents the position of the transducer connected to module 2. Thus the monitored weld is effectively partitioned into thirty-two sections on this display. A digital representation of flaw location (in inches) is presented after the rightmost square. For each indication that was detected during active monitoring, a new weld map is printed showing its type code, relative size, and relative location between transducers in the time of occurrance. The relative size of the indication is displayed as a two-place number representing the average energy content of the acoustic emission contributing to the detection of the indication.

Table 4.1 FLAW DISCRIMINATION MATRIX

	CRACK	IP	LOF*	POROSITY	UNCLASSIFIED
BURSTS/SEC	3	3	3	5	3
ENERGY RANGE	$100 \leq R \leq 1000$	$100 \leq R \leq 1000$	$100 \leq R \leq 1000$	$100 \leq R \leq 1000$	$100 \leq R \leq 1000$
LOCATION SIMILIARITY	0	0 (Pass 1 & 2)	0	2	0
ACTIVE FREQUENCY	270kHz	270kHz	920kHz	NONE	NONE

* An alternative algorithm may be based upon an energy range of $10 \leq R \leq 100$ and a characteristic frequency of 270 kHz.

```
OPERATION : RUN
PASS   5


OPERATION : DISPLAY
PASS   5

HULL NUMBER __________ DATE ___/___/_________

GRIN SETTINGS_________ WELD POSITION_________

ACTIVE MODELS (C,I,L,P,U):

    3:    1,  96-1008, 242,    0
    3:    1,  96-1008, 242,    0
    3:    1,  96-1008, 282,    0
    5:    1,  96-1008, 211,    2
    3:    1,  96-1008, 211,    0

REMARKS:
```

Figure 4.5 EXAMPLE OF PRINTED TEST DATA (Manual 36" Weld)

5.0 PRODUCTION LINE MONITORING

5.1 Data Acquisition

The previously described production line acoustic emission weld monitoring system was taken to the Lima Army Tank Plant (LATP) production facility for six months of production weld monitoring to quantify the accuracy of the AEWM by comparison of AE flaw indications to a combination of subsequent standard NDE tests.

Figure 5.1 shows the production line weld monitoring setup at the LATP. Monitoring was accomplished on a non-interference basis in the normal flow of weld production. The weld monitored was the sidewall to floor plate weld of the M1 tank hull: the outside weld at Work Station 1, and inside weld at Work Station 2.

All welding used the Metal Inert Gas (MIG) welding process. The welds are 229 in. in length. The root pass is done from the outside with the manual wire MIG welding process. The remaining outside weld is done semi-automatically in two steps: the first 139 in. are fully welded, then the back 90 in. are fully welded. Each part was separately monitored by acoustic emission. The inside weld is also done in two parts: a semi-automatic 193 in. weld and a 36 in. manual weld. Initially only the 193 in. weld was monitored (about 20 hulls). The long outside weld typically requires 10 passes; the short outside weld requires 3 passes; 3 passes are also required on both parts of the inside weld. A total of 25 hull welds (5000 feet of weld pass) were monitored during the six-month production test.

AE monitoring was performed on the hull at Work Stations 1 and 2; the hull then went to Work Station 3 for additional welding, and then to x-ray for examination.

AET 175L sensors were used for the production-line monitoring. Permanent magnet hold-down fixtures attached the sensors to the hull. Sensor placement was on the outside sidewall at Work Station 1 and on the inside sidewall at Work Station 2, to avoid interference with welder movement. Guard transducers were placed, as described in Section 4.2, to avoid acquisition of acoustic data from simultaneous, similar welding performed on the opposite side of the hull floor plate.

5.2 Data Base

Table 5.1 provides the flaw detection data for the twenty-five welds monitored. Key items presented are acoustic emission (AE) indications

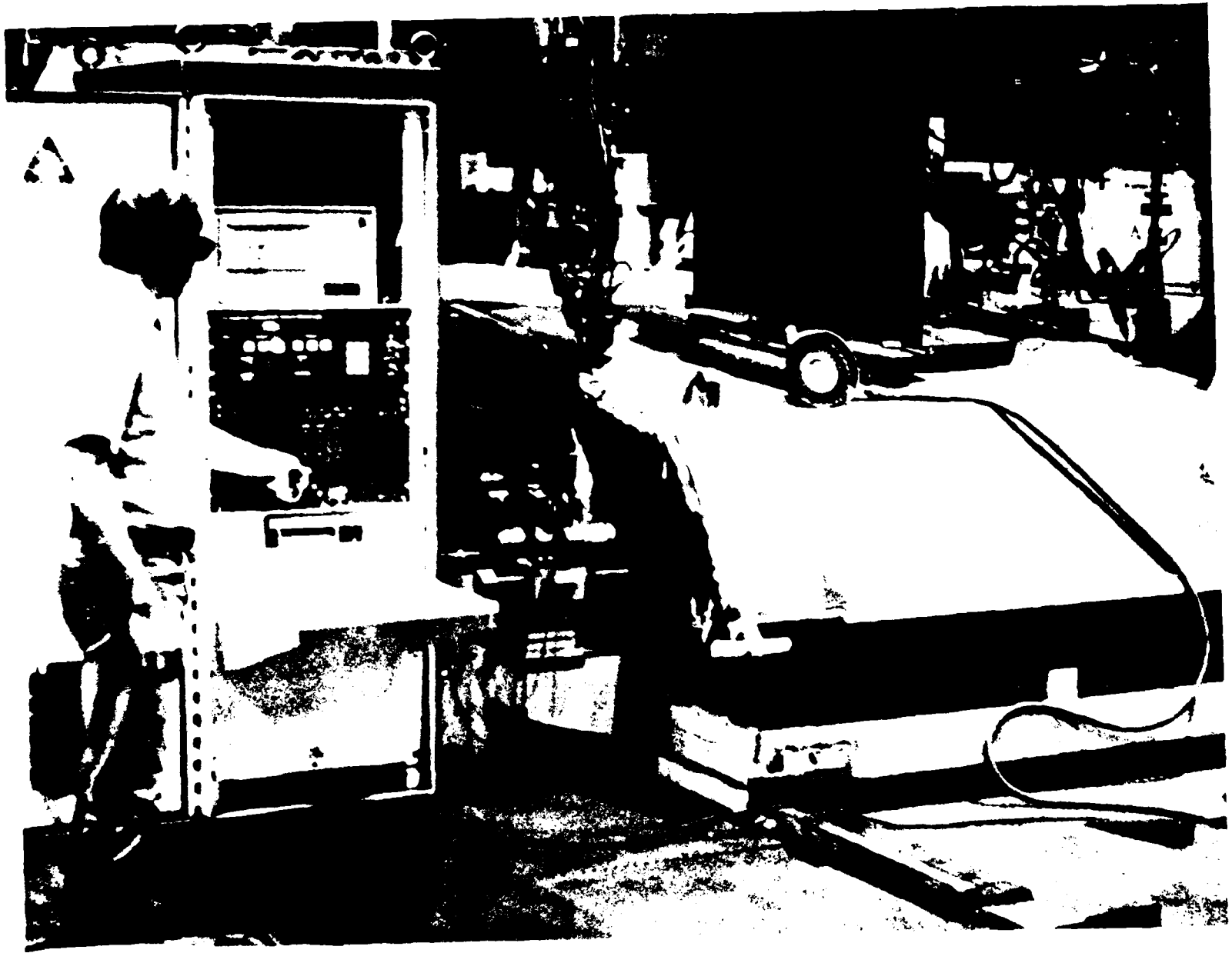

Figure 5.1 PRODUCTION LINE MONITORING

(per the algorithm used for flaw classification and sizing), x-ray/ ultrasonic confirmation, flaw type, disposition, and inspection personnel comments relative to test results. Disposition includes actual repairs performed and repairs which would have been performed if flaw detection had occurred on initial radiographic readings.

The following rules were applied during the development of the data base:

(a) A locational tolerance of 3 in. was allowed for an AE indication to be considered in agreement with an x-ray indication.(The reason for these limits is discussed in Section 5.3.2.)

(b) It was decided to re-examine the x-ray film and perform ultrasonic inspection in "questionable" areas where initial x-ray examination did not substantiate AE indications. The greatest discrepancy between AE/initial x-ray inspection data occurred for cracks (7 AE/3 x-ray). It was felt the potential cause of this discrepancy was that x-ray is a poor detector of cracks. General Dynamics NDT personnel re-examined the radiographs and performed ultrasonic inspection in the questionable areas. Their evaluation was considered final.

(c) Certain cracks were classified as "delayed". As monitoring progressed, it became evident, from post-weld radiography and ultrasonics, that the first 36 in. of the outside root pass had substantial transverse cracking. The AEWM did not detect flaws in this area. They were initially delayed crack suspects since (1) the larger cracks (1-1/2 in. and 2 in.) were open to the surface and had not been detected by the dye-penetrant inspection after the weld had been completed and prior to x-ray inspection, (2) they occurred in the hand welded nose weld areas historically suspect of delayed cracks, and (3) they were transverse in nature (i.e, cold cracks). Subsequent testing (described in Section 6) demonstrated such transverse flaws to indeed be delayed cracks.

Table 5.1 FLAW DETECTION DATA

HULL NO.	AE INDICATIONS	CONFIRMATION	FLAW	DISPOSITION	REMARKS
H-1420	-	X-Ray	1½" Crack (TV)	Repair	*
	-	X-Ray	2" Crack (TV)	Repair	*
	-	X-Ray	¼"(2),1½" Cracks (TV)	Repair	*
H-1426	-	-	-	Accept	Good Weld
H-1432	-	X-Ray	¼"(6)Cracks(TV)	Repair	*
H-1438	C2	X-Ray	1" Crack (TV)	Repair	Re-Read
	L2	X-Ray	1" LOF	Accept	Re-Read
H-1457	-	X-Ray	¼"(11)Cracks(TV)	Repair	*
H-1468	L4, L5	X-Ray	8" Porosity(Li)	Accept	-
	U2	X-Ray	1/8" Porosity (Lo)	Accept	-
H-1477	I9, I8(3)	X-Ray	¼" Crack (TV)	Repair	-
	I8(2), U8	X-Ray	¼"¼" Cracks(TV)	Repair	Re-Read
	-	X-Ray	4½" Porosity (Li)	Repair	AEWM Blinded
	U1	X-Ray	1/8"(3)Porosity (Lo)	Accept	-
H-1490	U2	X-Ray	¼" Porosity(Lo)	Accept	
	I9	X-Ray	Porosity(Li)	Accept	No UT Possible
	C3, C2	X-Ray	¼"(2)Cracks(TV)	Repair	-
H-1504	C3,L1,U1(2)	UT	½" Crack (TV)	Repair	Re-Examination
	I4	UT	Crack (TV)	Repair	Re-Examination
	I2	X-Ray	3" Incomplete Penetration	Accept	-
	C2	X-Ray	½" Crack (TV)	Repair	-

Li = Linear
Lo = Local
TV = Transverse Crack

C = Crack
I = Incomplete Penetration
L = Lack of Fusion

P = Porosity
U = Unclassified
* = Suspected Delayed Cracking or Hand Weld from Inside Which was not monitored with the AEWM

Table 5.1 FLAW DETECTION DATA (continued)

HULL NO.	AE INDICATIONS	CONFIRMATION	FLAW	DISPOSITION	REMARKS
H-1504 (cont)	P5 (5)	Repaired Prior to X-Ray	4"Porosity(Li)	Repair	-
	U2	X-Ray	1"Porosity(Lo)	Accept	-
H-1517	I3	—	—	Accept	No UT Possible
	I3, L4	X-Ray	1¼" LOF	Accept	—
H-1540	U3	X-Ray	5½"Porosity(Li)	Accept	
	I6	X-Ray	—	Accept	
H-1550	I5	X-Ray	1"(2)Cracks(TV)	Repair	
	U2, U3	X-Ray	2"Porosity(Li)	Accept	
	U3	X-Ray	2"Porosity(Li)	Accept	
	I5	X-Ray	1"Porosity(Li) Cracks	Repair	Re-Read
	I5,U4	X-Ray	2"Porosity(Li) Tailed Porosity Cracks	Repair	Re-Read
H-1553	I1,I4	X-Ray	½" Crack (TV)	Repair	
H-1568	C2	UT	Crack	Repair	Re-Examination
	—	X-Ray	3/8"(2) Cracks (TV)	Repair	**
H-1501	—	X-Ray	1"Crack (TV)	Repair	
H-1572	ELIMINATE HULL	FROM DATA BASE	GUARD CHANNEL NOT	WORKING	
H-1577	I3	X-Ray	½"Crack (TV)	Repair	
	Pass 1 - I2 Pass 3 - U3,C4 C1,C5, C2	X-Ray	3"Porosity(li) Tailed Porosity and ¼" Cracks	Repair	Re-Read
	—	X-Ray	½"C1)Crack(TV)	Repair	Re-Read

Li = Linear
Lo = Local
TV = Transverse Crack
** = Hand Welded Floor Cutout - Not Monitored

C = Crack
I = Incomplete Penetration
L = Lack of Fusion

P = Porosity
U = Unclassified
* = Suspected Delayed Cracking or Hand Weld from Inside Which was not monitored with the AEWM

Table 5.1 FLAW DETECTION DATA (continued)

HULL NO.	AE INDICATIONS	CONFIRMATION	FLAW	DISPOSITION	REMARKS
H-1589	_	X-Ray	½"Crack (TV)	Repair	*
	_	X-Ray	½"Crack (TV)	Repair	**
	_	X-Ray	3/8"Crack(TV)	Repair	**
H-1595	_	X-Ray	Porosity (Li)	Repair	
	I4	X-Ray	Gas Cavity Crack	Repair	Re-Read
H-1624	_	X-Ray	1"(7)Cracks(TV)	Repair	*Lost Passes
	_	X-Ray	1"(7)Cracks(TV)	Repair	*1&2 Defective
	_	X-Ray	1" Crack (TV)	Repair	*X-dcrCable
H-1634	I4	X-Ray	8" Incomplete Penetration	Accept	
	I1	X-Ray	1" Incomplete Penetration	Accept	
	_	X-Ray	½" Crack (TV)	Repair	*
	_	X-Ray	½" Crack (TV)	Repair	*
H-1645	I4 I4 U2 U3 U6	UT	Porosity Crack	Repair	No X-Ray Possible
	L2	X-Ray	1" Porosity(Li)	Accept	
H-1663	C5	X-Ray	½"(2)Cracks(TV)	Repair	Re-Read
	C4	UT	Crack (TV)	Repair	Re-Examination
	I6	X-Ray	½"Gas Cavity	Accept	
H-1687	I2	UT	Crack	Repair	No X-Ray Possible
	C1 I2	UT	Crack	Repair	No X-Ray Possible

Li = Linear
Lo = Local
TV = Transverse Crack
** = Hand Welded Floor Cutout-Not Monitored

C = Crack
I = Incomplete Penetration
L = Lack of Fusion

P = Porosity
U = Unclassified
* = Suspected Delayed Cracking or Hand Weld from Inside Which was not monitored with the AEWM

Table 5.1 FLAW DETECTION DATA (continued)

HULL NO.	AE INDICATIONS	CONFIRMATION	FLAW	DISPOSITION	REMARKS
H-1707	L5	X-Ray	1"Porosity(Li)	Accept	
	I1	X-Ray	6"Incomplete Penetration	Accept	
	I1	X-Ray	15" Incomplete Penetration	Accept	

Li = Linear
Lo = Local
TV = Transverse Crack

C = Crack
I = Incomplete Penetration
L = Lack of Fusion

P = Porosity
U = Unclassified
* = Suspected Delayed Cracking or Hand Weld from Inside Which was not monitored with the AEWM

The resultant production line monitoring data base as defined by radiography and ultrasonics showed 43 "in-process" flaws, 41 delayed cracks, and 4 tack-weld cracks.*

5.3 Data Analysis

The following narrative discusses AE production monitoring in terms of detection, location, characterization, sizing, and accept/reject accuracies relative to production x-ray, x-ray re-read, and follow-up ultrasonic results. The analysis was made subject to the following:

(a) We ignore the suspect delayed cracks (marked with an * in the remarks column in Table 5.1), since there would have been no AE monitoring when they occurred, per Section 5.1.

(b) Unmonitored cracks in tack-welds are ignored.

(c) When there are multiple flaw-type calls by the AEWM for the same defect, the most critical flaw characterization is used (crack> porosity> incomplete penetration> lack of fusion> unclassified).

5.3.1 Flaw Detection

Table 5.2 lists AE indications vs. initial x-ray inspection results. The table shows that 58 percent (25/43) of the AE indications were confirmed by initial x-ray inspection, with 3 undercalls. (Note: there is no way to reliably arrive at the summary numbers at the bottom of the table from the matrix of numbers above them, because there is not always a one-to-one correspondence between data as presented on the left and on the right in the table).

Table 5.3 provides "thresholded" AE indications vs. repairs (based upon General Dynamics production radiographic interpretation of specific types and sizes of defects for repair purposes, per Material Review Board). AE thresholding is based upon the fact that a relative measurement of acoustic energy released from each weld flaw is provided by the AEWM with each weld flaw characterization. Thus energy-related flaw severity cutoffs can be used to provide a viable measure of correlation between AE, radiography, and repair. The rejectable AE flaw type/size thresholds used were selected by manual data review to provide the best results. With this sort, of the 10 actual repairs, AE identified 50 percent (5/10).

---

* spot welds put in to hold assembly together prior to production welding (hence unmonitored by AE)

Table 5.2 AE INDICATIONS VS. INITIAL X-RAY

AE					X-RAY	
C	I	L	P	U	# INDICATIONS	TYPE
2	4	-	-	-	7	C
-	5	-	-	-	5	IP
-	1	-	-	-	1	LOF
-	1	3	1	3	10	P(Li)
-	1	-	-	4	5	P(Lo)
7	10	1	-	-	-	**

25/43 AE Indications Confirmed with 3 Undercalls

Table 5.3 AE INDICATIONS* VS. INITIAL REPAIRS

AE					REPAIRS	
C	I	L	P	U		TYPE
2	2	-	-	-	7	C
-	-	-	-	-	-	IP
-	-	-	-	-	-	LOF
-	-	-	1	-	3	P(Li)
-	-	-	-	-	-	P(Lo)
7	1	-	-	-	-	**

5/10 AE Indications* were Repairs with 5 Undercalls

* Only P
C
I > 4

** Overcalls

The above 58 percent flaw detection and 50 percent repair detection accuracies can be re-evaluated by subsequent re-examination of the AE-indicated flaw areas not identified with flaws on initial x-ray reading. It was decided to (a) re-examine the x-ray film, and (b) perform follow-up ultrasonic inspection in these "questionable" areas. Table 5.4 presents a summary of the results of AE indications vs. initial x-ray, x-ray re-examination, and ultrasonic inspection results. The acoustic emission flaw detection confirmation is raised to 93 percent (40/43) with3 undercalls. In several cases in these tables, there is a flaw-type re-classification. For instance, initial x-ray would call a defect "porosity", re-read of x-ray and/or follow-up ultrasonic showed cracks in the same area. Our subsequent analysis changed the flaw identification from the less critical initial "porosity" to the more critical "crack" on re-read.

AE type/size related cutoffs can again be used to provide a workable means of determining the correlation between AE indications and accept/reject for the Table 5.4 data base. The cutoffs used for repair indications were: all C, all P, and all I>3 (almost identical to those in Table 5.3). Table 5.5 presents the results using these cutoffs. We defined repairs in this case as those which had been made or would have been made if the flaw would have been found on initial x-ray reading. The table shows AE indication correlation for the 23 repairs is 83 percent as 19/23 repairs were identified by AE with 4 overcalls.

5.3.2 Flaw Location

Flaw location is carried out with one sensor at each end of the weld. The actual location of the acoustic event is computed by the time difference of arrival of the AE signal at each of the sensors. AE flaw location "error" can be induced by (a) hardware/software in the Weld Monitor itself, (b) variance in sensor placement on the hull, and (c) variance in x-ray film placement on the hull. The AEWM can,in theory, locate flaws to within +/- 1 in. It was estimated that sensor placement on the hull was within +/- 1 in., and that reliability of x-ray film location on the hull was also +/- 1 in. Simply adding the three sources of error provides potential locational inaccuracy of +/- 3 in. This +/- 3 in. accuracy was used as a window in developing the above data base, as mentioned earlier.

Table 5.6 provides a list of AE flaw locations vs. x-ray flaw locations, for flaws where location was recorded by both AE and x-ray. The table shows, if we mathematically average the absolute variation in locational inches (37 in./43 flaws), that the AEWM provides better than 1 in. average accuracy in flaw location.

Table 5.4 AE INDICATIONS VS. X-RAY/UT

AE					X-RAY/UT	
C	I	L	P	U	# INDICATIONS	TYPE
9	11	-	-	-	21	C
-	5	-	-	-	5	IP
-	1	1	-	-	2	LOF
-	1	3	1	3	10	P(Li)
-	1	-	-	4	5	P(Lo)
-	3	-	-	-	-	**

40/43 AE Indications Confirmed with 3 Undercalls

Table 5.5 AE INDICATIONS* VS. INDICATED REPAIRS

AE					REPAIRS	
C	I	L	P	U		TYPE
9	9	-	-	-	20	C
-	1	-	-	-	-	IP
-	0	-	-	-	-	LOF
-	2	-	1	-	3	P(Li)
-	-	-	-	-	-	P(Lo)
-	1	-	-	-	-	**

19/23 AE Indications* were Repairs with 4 Undercalls

* Only P
C
I > 3

** Overcalls

Table 5.6 FLAW LOCATIONS

FLAW NO.	BY AE	BY X-RAY	DIFFERENCE
1	64 in.	64 in.	0 in.
2	48 in.	48 in.	0 in.
3	92 in.	93 in.	-1 in.
4	105 in.	105 in.	0 in.
5	28 in.	28 in.	0 in.
6	102 in.	99 in.	+3 in.
7	94 in.	94 in.	0 in.
8	64 in.	64 in.	0 in.
9	30 in.	32 in.	-2 in.
10	2 in.	4 in.	-2 in.
11	64 in.	63 in.	+1 in.
12	78 in.	77 in.	+1 in.
13	96 in.	93 in.	+3 in.
14	132 in.	134 in.	-2 in.
15	144 in.	142-146 in.	0 in.
16	126 in.	127 in.	-1 in.
17	94-96 in.	93 in.	-1 in.
18	30 in.	28-33 in.	0 in.
19	130 in.	131 in.	-1 in.
20	64 in.	64-66 in.	0 in.
21	2 in.	3-5 in.	-1 in.
22	50 in.	51 in.	-1 in.
23	90 in.	88 in.	+2 in.
24	130 in.	132 in.	-2 in.
25	46 in.	44 in.	+2 in.
26	36 in.	33 in.	+3 in.
27	96 in.	94 in.	+2 in.
28	78 in.	78 in.	0 in.
29	94 in.	89-96 in.	0 in.
30	46 in.	45 in.	+1 in.
31	130 in.	130 in.	0 in.
32-34	128-130 in.(3)	128-132 in.	0 in.
35	80 in.	82 in.	-2 in.
36	20 in.	20 in.	0 in.
37	132 in.	131 in.	+1 in.
38	86 in.	86 in.	0 in.
39	132 in.	131 in.	+1 in.
40	46 in.	46 in.	0 in.
41	130 in.	130 in.	0 in.
42	92 in.	93 in.	-1 in.
43	48 in.	45-60 in.	0 in.
			-----
			37 in. Absolute

5.3.3 Flaw Characterization

For this analysis we use Table 5.1, it is the best data base for characterization evaluation because it is the largest and includes 3 standard NDE inputs (x-ray, re-read x-ray, and ultrasonics) for confirmation of AE indications. The table shows for flaws identified by the Weld Monitor as:

Crack - The AE classification model is 100 percent accurate in calling cracks correctly (9/9).

Incomplete Penetration - The model is 23 percent accurate when calling incomplete penetration (5/22); it is 100 percent accurate in calling incomplete penetration (5/5).

Lack of Fusion - The model is 25 percent accurate when calling lack of fusion (1/4); it is 50 percent accurate in calling lack of fusion (1/2).

Porosity - The model is 100 percent accurate in calling repairable porosity correctly (1/1).

Unclassified - The model indicates acceptable porosity 100 percent of the time (7/7).

5.3.4 Flaw Sizing

The AEWM's ability to size flaws is addressed in the following tables, which plot standard NDT-indicated flaw size against AEWM severity for each of the AEWM flaw-type indications. This was done for flaws which had size recorded.

AE Indication: C

Figure 5.2 is a plot of all "C" AE indications. In this case, they all happen to be cracks by standard NDT definition. The figure shows "actual" crack size vs. the C-related AE intensity number. Severity numbers seem to be independent of crack size. Based on data from the delayed cracking study as presented in Section 6, this relationship is due to the ringdown count windowing (96-1008) used in the production monitoring AE model. The AEWM is apparently looking at tails of

AE signals and not at peaks from these "macro" cracks. It is expected that raising the top of the energy window (i.e., 1008-4080), will allow the intensity number to provide a better indication of macro-crack size.

AE Indication: U

Figure 5.3 is a plot of all U indications. They all appear to be acceptable (small) porosity by standard NDE definition. There seems to be a rough relationship between intensity number and size of these porosities. This is probably due to the detection of micro-cracking associated with the porosity (i.e., more porosity, larger micro-cracking). The low energy released during micro-cracking is within our model window (96-1008), thus flaw sizing is realized.

AE Indication: I

In Figure 5.4 we see that the intensity numbers for cracks as defined by standard NDE show a flaw size flatness similar to Figure 5.2 for cracks.

This is to be expected since I is the same model as C (except for pass number). Both do 100 percent in identifying cracks as "Cracks". The independence of severity number appears to be due to the previous explanation: the "C" severity numbers' insensitivity to crack size.

The intensity numbers from incomplete penetration, as defined by standard NDT, do not give any correlation to flaw size. The non-correlation with size is conjectured as due to the fact that these AE indications are from small cracks at the ends of the incomplete pentration, while the sizes plotted are the actual extent of the incomplete penetration itself. Note, these indications are mostly low numbers (4 of 5 have an intensity number of 2 or less), lending credence to the presence of small cracks, and thus further support our micro-crack hypothesis presented above.

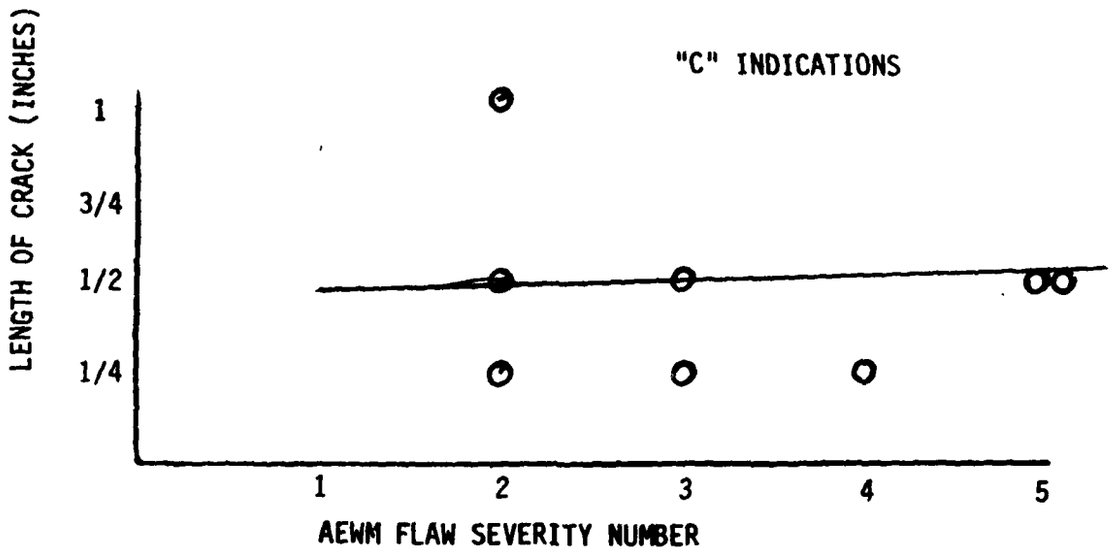

Figure 5.2 LENGTH OF CRACK VERSUS AEWM SEVERITY NUMBER

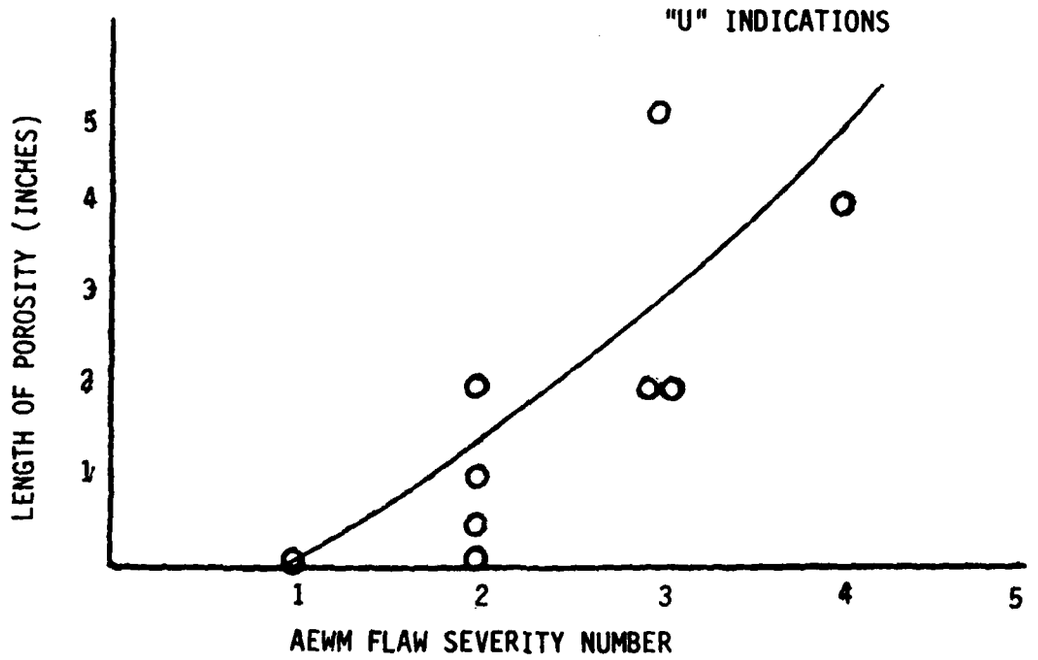

Figure 5.3 LENGTH OF POROSITY VERSUS AEWM SEVERITY NUMBER

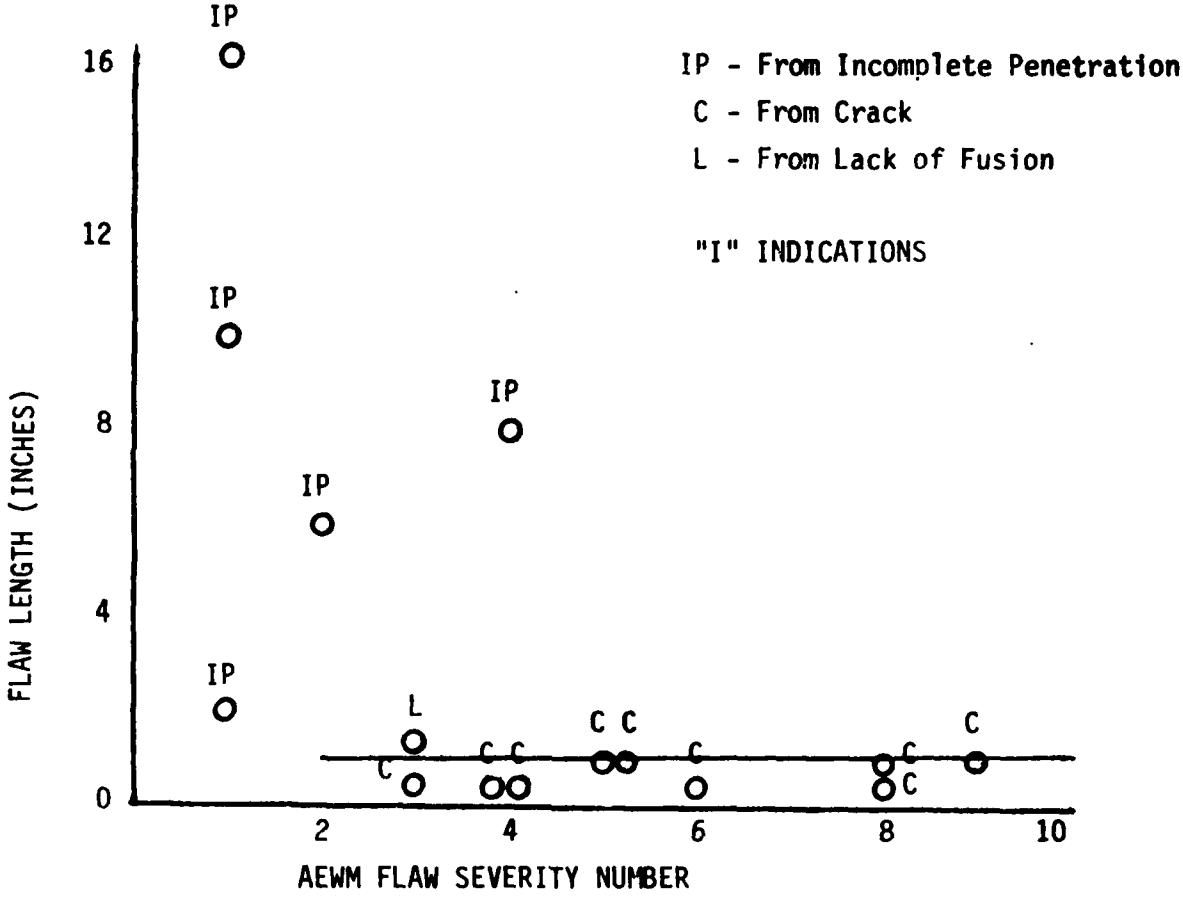

Figure 5.4 LENGTH OF INCOMPLETE PENETRATION VERSUS AEWM FLAW SEVERITY NUMBER

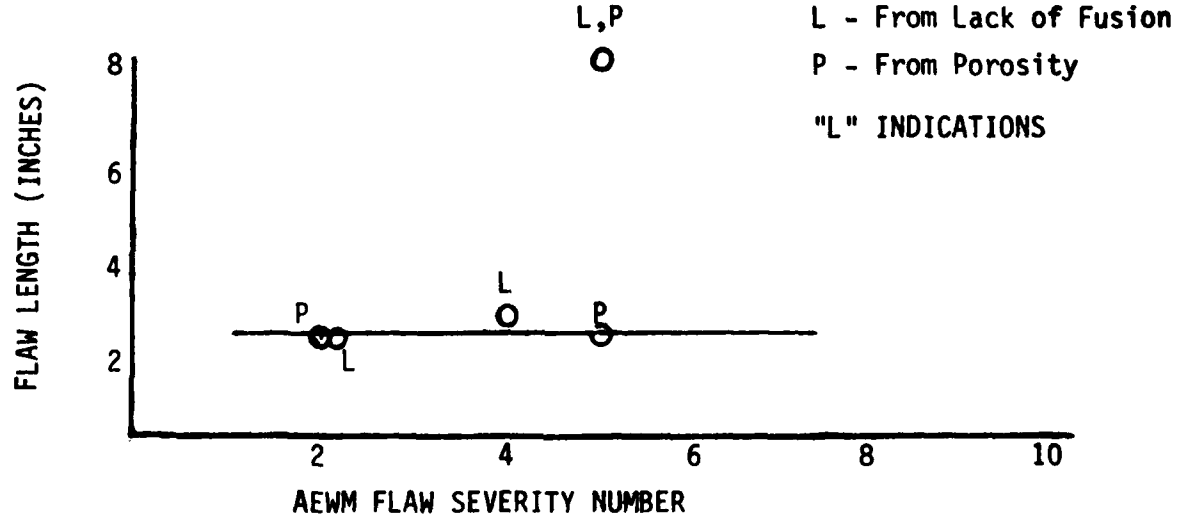

Figure 5.5 LENGTH OF LACK OF FUSION VERSUS AEWM SEVERITY NUMBER

AE Indication: L

In Figure 5.5 we may be seeing the same severity insensitivity to size as in Figure 5.2 for cracks, but more of a spread as to flaw size actually measured (as per I above). We have a limited L data base from which to draw conclusions; however L may respond more to macro-cracks then I.

AE Indication: P

An analysis of the P severity number vs.indication size is not possible because there is only one data point.

Figures 5.2 through 5.5 summarize the AE sizing results with the software model which was used. They show that the U severity sizes scattered acceptable porosity in the range of 1/8 in. to 2 in. in length. In retrospect, this is not surprising since the U model is the same as the P (porosity) model except for rate and locational tolerance (5:1 vs 3:1 and 2 vs 0). U indications come from small porosities, while P indications come from the larger, repair-requiring porosities (1 in. to 4.5 in.). Incomplete penetration is detected by low level AE due to isolated, localized crack-type signatures at the flaw tips. The upper windowing used (1008) caused problems in sizing macro-cracks.

5.3.5 Accept/Reject

This discussion relates to the data presented in Table 5.5 where repairable flaws are indicated by an AE characterization and sizing sort on the data presented in Table 5.4.

Table 5.7 shows how the Table 5.5 numbers can be improved by reclassification of 4 flaw indications. If follow-up UT confirmation could have been made on one more flaw (originally analyzed as unconfirmed) the repair identification could be raised to 87 percent (20/23) with 3 overcalls and 3 undercalls (such follow-up UT confirmation was made successfully in 15 of 15 other cases). If we assume that the one TV crack missed by the AEWM was a delayed crack (i.e., not monitored) we decrease our undercalls to 2. Finally, if we had used a higher upper energy window in the P model, as follow-up laboratory data analysis verified, we would have picked up the 2 AE-missed porosity repairs. Our repair identification accuracy would then rise to 88 percent, with 12 percent overcall and 0 percent undercall.

TABLE 5.7 RECLASSIFICATION OF AE FLAW INDICATIONS

ASSUMPTION	SOFTWARE	AE REJECTS	RESULTANT REPAIRS	AE OVERCALLS	AE UNDERCALLS
Present Results	Current Model	23	19	4	3
Confirmed Flaw	Current Model	23	20	3	3
Delayed Crack	Current Model	23	20	3	2
Higher Porosity Window	New Model	25	22	3	0

6.0 DELAYED CRACK INVESTIGATION

A meeting was held at LATP to review the weld monitoring progress. In attendance were personnel from TACOM, GDLS, and GARD.

In reviewing the data, general agreement was reached that the AEWM was correlating well with x-ray and ultrasonic test results. It was decided that one area (nose section slope weld) was a problem to be addressed during the remaining weld monitoring time available on the program.

In an attempt to help resolve whether the nose section cracks were delayed cracking, unmonitored, or simply AEWM missed flaws, the long outside weld (Station 1) was monitored during welding and post-welding, for as long a time period as production would allow. The hull was then moved to Station 2 where the inside hand welding of the nose slope weld (the weld of interest) was monitored. Post-weld monitoring was also done after completion of all inside welding. Post-weld monitoring was continued until production required the hull's removal. In addition, some nose welds were post-weld monitored in Station 3, where the glacis plate and nose section welding are completed.

6.1 Delayed Crack Occurrence Verification

Initially, four hulls (1712-1728) were monitored to optimize the system gain levels required to (a) monitor inside manual welding, (b) monitor outside manual root pass welding, and (c) post-weld monitor the nose slope weld (both outside and inside). Table 6.1 provides the flaw detection data for these four hulls. Four welds were monitored, both during and post weld, over a range of system gain levels, to optimize gain settings for subsequent monitoring. It was determined that the current system gain settings were good. The one real-time flaw produced (crater crack) was missed by the AEWM because system gain was reduced by 9db at the time the flaw occurred.

An additional four hulls (numbers 1734-1889) were then monitored with the AEWM to look for delayed cracking. The signal processing algorithm for this work was the same used for the 6 month production line test described in Section 5. The test parameters were as follows: *

C - Crack 3:1, 96-1008, 242, 0

I - Incomplete Penetration 3:1, 96-1008, 242, 0

L - Lack of Fusion 3:1, 96-1008, 282, 0

* as defined in Section 4.0

Table 6.1 FLAW DETECTION DATA (Gain Optimization)

HULL NO.	AE INDICATIONS	FLAW	CONFIRMATION	DISPOSITION	REMARKS
H-1712	–	–	—	—	Right inside manual weld -6db gain Left inside manual weld normal gain
H-1715	—	—	—	—	Right inside manual weld normal gain Left inside manual weld -9db gain
H-1724	—	—	—	—	Right inside manual weld normal gain Left inside manual weld -6db gain
H-1728	— —	Crater Crack —	Welder(visual) —	Repair —	Right side manual weld -9db gain Left side manual weld -13db gain
					All above welds were PWM for 2 hours

Li = Linear
Lo = Local
TV = Transverse Crack
WP = Weld Pass
LOW = Long Outside Weld
LIW = Long Inside Weld

C = Crack
I = Incomplete Penetration
L = Lack of Fusion

P = Porosity
U = Unclassified
* = Suspected Delayed Cracking
PWM = Post-Weld Monitoring

P - Porosity 5:1, 96-1008, 211, 2

U - Unclassified 3:1, 96-1008, 211, 0

Table 6.2 provides the flaw detection data for the four welds monitored. Key items presented are acoustic emission indications, x-ray/ultrasonic confirmation, flaw type disposition, and post-weld monitoring time when delayed crack AE indications occurred.

The following paragraphs discuss the Table 6.2 AE delayed crack indications with respect to standard NDE confirmation results. (The analysis does not include the "real-time" flaws in Hull No. H-1734.) Table 6.3 summarizes the results.

Hull No. 1734 did have 2 TV cracks in the nose slope section that were not detected by AE. It is expected these were simply unmonitored when they occurred, since post-weld monitoring was done for only 1 hour. Hull No. 1748 did not have TV cracks or other rejectable flaws, as determined by x-ray. There were no AE indications from the welds.

At Work Station 2, Hull No. H-1824 gave delayed crack indications that were verified by follow-up UT inspection: after about 1 hour of post-weld monitoring, 9 flaw indications were recorded from 1 location at 113 inches from Sensor 1 (within about 5 minutes, as a cluster). Welder activity at this time consisted of pre-heating the nose section of the hull. This area is part of the weld being monitored; the indications were from the opposite end of the weld. An additional 7 AE indications appeared after about 2 hours of post-weld monitoring (4 from the above 113 location and 3 others at 144 inches from Sensor 1). These events were our first AE production line results showing that delayed cracking does indeed occur. A real-time AE indication was observed, during welding of the long inside weld, from the same area that delayed cracking was detected earlier.

Post-weld monitoring of Hull No. H-1889 (at Work Station 1) also gave delayed crack indications. After about 1/2 hour of post-weld monitoring, 2 flaw indications were recorded from a location 64 inches from Sensor 1. Additional AE crack indications at the 64 inch location were recorded after 44 and 50 minutes, and 11-1/2 hours, of post-weld monitoring. At 4-1/2 hours, a delayed crack indication was recorded at 132 inches. Unfortunately there was no x-ray or UT confirmation of the Hull No. H-1889 potential delayed cracks, since additional fabrication work was done on the hull in the areas of interest before radiography or ultrasonic testing could be performed. These AE indicated crack areas were not in the nose slope area where most TV cracks have occurred.

Table 6.2 FLAW DETECTION DATA (Occurrence Verification)

HULL NO.	AE INDICATIONS	FLAW	CONFIRMATION	DISPOSITION	REMARKS
1734	—	3/4" TV Crack	X-Ray	Repair	*
	—	3/4" TV Crack	X-Ray	Repair	*
	LOW (Real-Time):				
	RP U4 (114")	Porosity (Li) (115")	X-Ray	Accept	
	WP1 L4 (112")				
	WP3 U1 (64")	1-1/2" Crack Cluster (64")	UT	Repair	
	C2(2) C3				
	WP8 C1 (64")				
	WP9 C1 (64")				
	SOW (Real-Time):				
	WP1 I5 (78")	1/2" (2) Crack (TV) (76")	X-Ray	Repair	
	WP2 U6 (96")	Porosity (Lo) (96")	X-Ray	Accept	
	No PWM Indications				Sta.1:1 hr. Sta.2:2 hr.
1748	No PWM Indications	—	X-Ray	Accept	Sta.1:1 hr. Sta.2:2 hr.
1824	PWM (Sta.2):				
	I5 (2) (113")	Crack (TV)(112")	UT	Repair	∿ 1 hr.
	U5				∿ 1 hr.
	I4 (3) (114")				∿ 1 hr.
	U3				∿ 1 hr.
	U4				∿ 1 hr.
	U1				∿ 1 hr.
	I4 (3) (112")				∿ 2 hr.
	L6				∿ 2 hr.
	I1 (144")	Crack (TV)(144")	UT	Repair	∿ 2 hr.
	I1				∿ 2 hr.
	I4				∿ 2 hr.
	End PWM				∿ 2 hr.

Li = Linear
Lo = Local
TV = Transverse Crack
WP = Weld Pass
LOW = Long Outside Weld
LIW = Long Inside Weld

C = Crack
I = Incomplete Penetration
L = Lack of Fusion
RP = Root Pass
SOW = Short Outside Weld

P = Porosity
U = Unclassified
* = Suspected Delayed Cracking
PWM = Post-Weld Monitoring

Table 6.2 FLAW DETECTION DATA (Occurrence Verification) continued

HULL NO.	AE INDICATIONS	FLAW	CONFIRMATION	DISPOSITION	REMARKS
1824 (con't)	LIW (Real-Time):				
	I7 (112")				Reactivation
H-1889	PWM (Sta.1):				
	C2, (64") L2		No X-Ray or UT Possible		∿ ½" hr.
	C2 (64")				∿ 1 hr.
	C1 (64")				∿ 1 hr.
	C7 (132")		No X-Ray or UT Possible		∿ 4½ hr.
	C2 (64")				∿ 11½ hr.
	End PWM				∿ 16½ hr.

Li = Linear
Lo = Local
TV = Transverse Crack
WP = Weld Pass
LOW = Long Outside Weld
LIW = Long Inside Weld

C = Crack
I = Incomplete Penetration
L = Lack of Fusion
RP = Root Pass
SOW = Short Outside Weld

P = Porosity
U = Unclassified
* = Suspected Delayed Cracking
PWM = Post-Weld Monitoring

Table 6.3 VERIFICATION MONITORING SUMMARY

HULL NO.	HOURS MONITORED		AE INDICATED DELAYED CRACKS		
	Outside Weld	Inside Weld	Outside Weld	Inside Weld	DELAYED CRACK CONFIRMATIONS (STD. NDT)
H-1734	1	1	0*	0	2
H-1748	1	2	0	0	0
H-1824	-	3	—	1 @ 1 hr 1 @ 1 hr	1 1
H-1889	16-1/2	-	1@ 1/2 to 11-1/2 hr. 1@ 4-1/2 hr.	—	No Confirmation Possible

* Expect post-weld monitoring time not long enough

However, they were in areas where suspect delayed cracks did occur, as confirmed by radiography during our six month production test.

It was noted during real-time monitoring of Hull H-1889 by AEWM operator observation of the AEWM LED display, that after weld pass 4 there were extensive amounts of low energy, high rate activity (described in Section 6.2.2) . This activity continued thru weld pass 10. This was our first production line indication of a possible "precursor" to delayed cracking.

This 4 hull test demonstrated that delayed cracks occur and that the AEWM can detect them. Based upon these favorable results an extended test was initiated to study the delayed crack problem. This delayed crack test program consisted of weld and post-weld monitoring of:

1. weld samples in the GD/MM&T weld lab, and

2. long outside hull welds, in production.

The following sections describe these efforts.

6.2 Laboratory Study

The laboratory study was performed in order to take a close look at the delayed crack problem under controlled conditions. A trial lab test was performed first. This was followed by a data analysis to permit change in the software flaw model to optimize on-line detection of delayed cracking.

6.2.1 Sample Description

The welding geometry used for the delayed crack laboratory experiments is shown in Figure 6.1. The weld geometry consisted of a single vee (60 degree included angle) butt weld. The bevel is shown in cross-section in Figure 6.2 along with a pass map and welding parameters found optimal (as determined by GD) for Gas Metal Arc welding in armor plate material.

Figure 6.3 shows the test setup in General Dynamic's MM&T Weld Laboratory. Figure 6.4 shows a close-up of a typical test plate with the AE sensors attached at each end of the weld.

A total of 12 weld specimens were fabricated by GD personnel and monitored with the AEWM. Four were fabricated from 12 inch wide, 1-1/2 inch thick, 37 inch long plates, with plate sides tack-welded to the weld table to provide restraint to produce delayed cracking. Two, made from 6 inch wide, 1-1/2 inch thick, 37 inch long plates, were fabricated

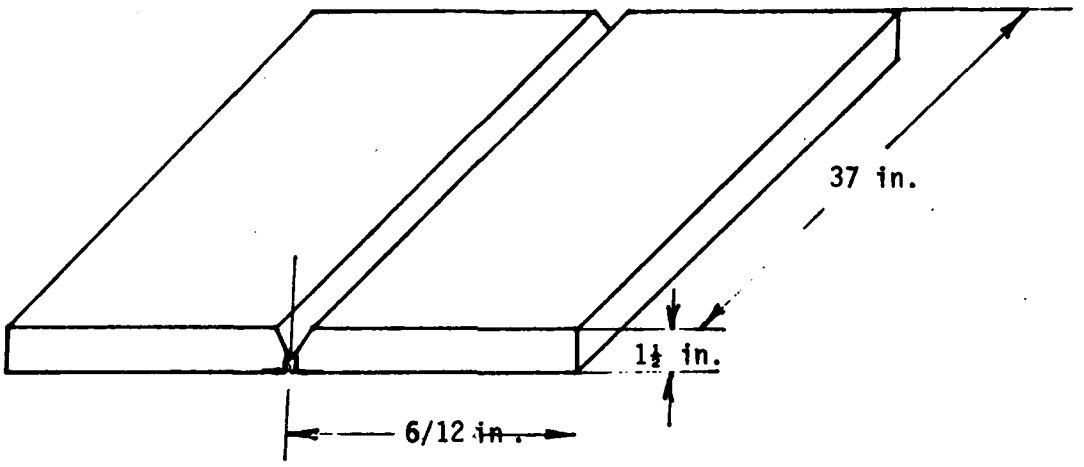

Figure 6.1 LABORATORY WELD JOINT DESIGN

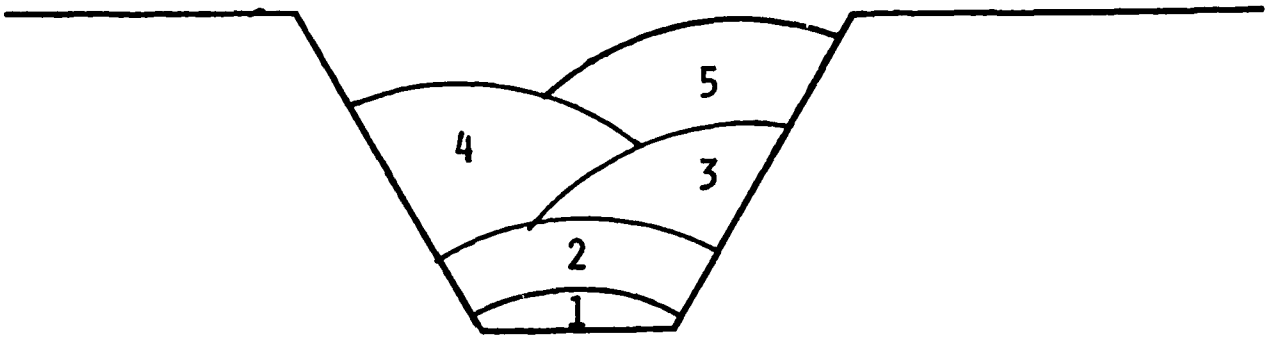

WELDING PARAMETERS

PASS	AMPS	VOLTS	TRAVEL SPEED	
1	300	26	13½ ipm	
2	300	26	13½ ipm	
3	300	26	13½ ipm	
4	300	26	13½ ipm	
5	300	26	13½ ipm	

Figure 6.2 WELD BEVEL AND PARAMETERS FOR AE DELAYED CRACK LABORATORY WELDS

Figure 6.3 TEST SET UP FOR AE DELAYED CRACK SIMULATION EXPERIMENTS

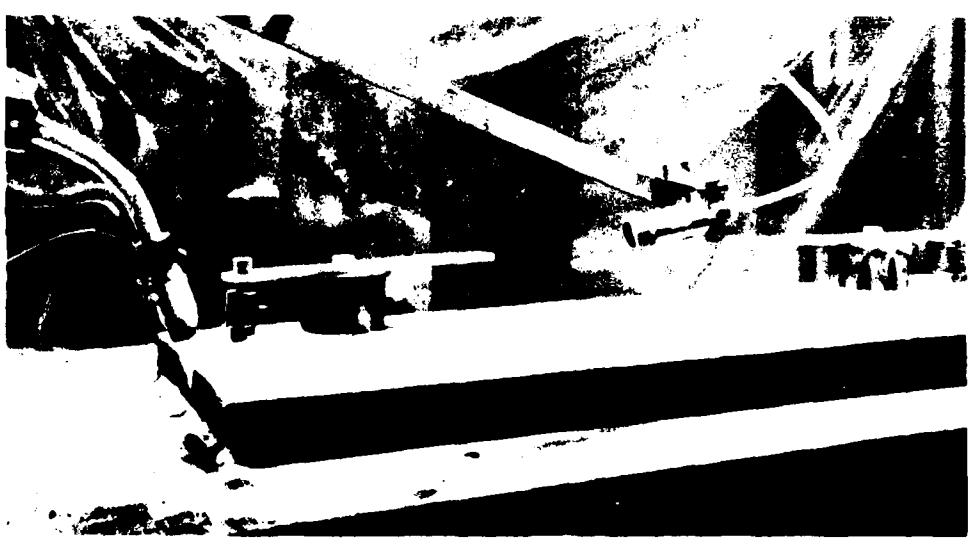

Figure 6.4 CLOSE UP OF WELD PLATES WITH AE SENSORS ATTACHED

after fastening the plates to the weld table with 1-1/2 inch bolts to eliminate the labor intensive task of air-arcing needed to remove the tack-welded plates after welding. The last 6 were fabricated from 6 inch wide by 37 inch long by 1-1/2 inch thick armor plates, with plate sides tack-welded to the weld table.

The 12 inch wide plates gave spurious AE indications from bad tack-welds, which due to geometric considerations, were located by AE at 0 inch to 10 inches from both ends of the test plate. Our GUARD Transducers, used on the production line, could not be used on the small plates in the weld lab to eliminate this effect. Thus, this restraint approach was abandoned. The bolted method of plate restraint was not sufficient to hold the plates to the weld table: they moved with the weld head position during welding and produced false AE indications. The last six 6 inch tack welded plates did not show the problem and their results are presented here. Typically, five passes were required to provide sufficient restraint in the weld to produce delayed cracks. The delayed cracking was induced by putting small amounts of hydrogen (H_2), over a range of 0.10 percent to 1.0 percent, into the shield gas. This concentration is realistic in terms of actual naturally occurring production flaws: a common source of delayed cracking is the result of insufficient pre-heat to remove all the moisture, the source of hydrogen prior to welding. Figure 6.5 is an x-ray of a weld section with a typical H_2-induced delayed crack.

6.2.2 Laboratory Test Results

The acoustic emission instrumentation used on this task was the AEWM system used in the previous tests. Radiography and penetrant testing were used to confirm flaws and provide corroborating evidence to correlate with AE results. Table 6.4 summarizes the results. Key items presented are total confirmed flaws induced, flaws detected by AE, and AE indication (real-time, precursive activity, delayed crack). Real-time as used in this analysis means the AE crack indication occurred during welding. Delayed crack means the AE indication occurred after welding was completed.

There were 30 TV cracks confirmed by radiography; AE detected 26 of them, for an 87 percent hit rate. X-ray-confirmed delayed cracks occurred in Plate No. 2 (0.15 percent H_2) only: the first occurred approximately 3 minutes after Weld Pass 2 was completed, and was detected by the AEWM; the second occurred 4 hours and 56 minutes after weld completion, and was also AEWM-detected. Both were in the same location There were 4 AE indications which were not confirmed by radiography.

There were 4 AE-missed cracks. Two, from the second third of the Plate No. 1 weld, were probably missed due to the large number of flaws

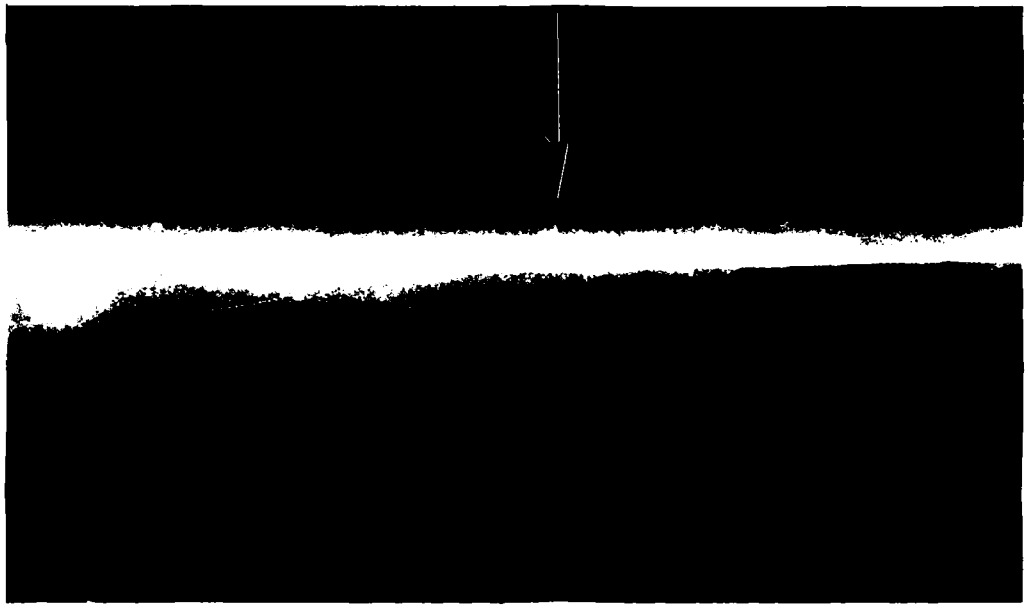

Figure 6.5 X-Ray of a Weld Section with a Hydrogen Induced Delayed Crack

Table 6.4 WELD LABORATORY AE DETECTION OF TRANSVERSE CRACKS

PLATE NO.	TOTAL CONFIRMED INDUCED FLAWS	AE DETECTED	AE INDICATION		
			REAL-TIME CRACK	PRECURSIVE ACTIVITY	DELAYED CRACK
1	7	5	5*	Yes	1*
2	5	4**	1	Yes	3
3	6	6	0	No	0
4	6	6	0	No	0
5	4**	3	3	No	0
6	2	2	2	No	0

* 1 Flaw site gave both real-time and delayed AE.

** 1 flaw shown to be outside transducer range thus originally not indicated.

NOTE: Missed 2 flaws in Plate No. 1 because of high acoustic activity

induced in the first 1/3 of the weld, which filled the AEWM memory. The other 2 missed were in Plate No. 2. One occurred outside of the transducer placement. It, as follow-up laboratory data analysis confirmed, was automatically rejected as an AE indication by the AEWM. The other, a missed TV crack, could have been simply unmonitored when it occurred: post-weld monitoring was done for 5 hours and there was still AE activity when the test was terminated.

It was noted from the AEWM LED lights during post-weld monitoring (both interpass and after completion of welding) that there were extensive amounts of low energy, high rate AE activity coming from Plate No. 2. Subsequent analysis of Plate No. 2 recorded data, at GARD, showed this low energy AE activity could be located, in the areas where the detected delayed cracks occurred, by reducing the "L" model window to 16-80 from 96-1008. This low energy, high rate AE activity is probably due to extensive micro-cracking (which was the result of hydrogen charging) and is probably the precursor to delayed cracks.

Of the 6 plates monitored 2 exhibited this precursive high rate activity. Plate No. 2 had extensive such activity after welding; Plate No. 1 had less. One delayed crack indication was obtained in Plate No. 1 after 2 hours of post-weld monitoring in an area where a TV crack was detected by radiography. The other 4 plates did not exhibit this precursive activity, and provided no delayed crack indications (i.e., all AE crack indications occurred during welding). Thus, monitoring for post-weld low energy, high rate AE activity may be a good indicator of potential delayed crack problems.

6.2.3 New Algorithm

Analysis of the recorded data, at GARD, showed that the production-used AE algorithm should be altered in the L, I, and P models to allow detection and classification of precursive activity and delayed cracks (L and I), and better porosity detection (P). The new algorithm was optimized as follows:

C = 3:1,	96-1008,	242, 0 *
I = 3:3,	96-4080,	242, 0
L = 7:1,	16-80,	211, 0
P = 5:1,	96-4080,	211, 2
U = 3:1,	96-1008,	211, 0

* as defined in Section 4.0

Rationale for these numbers is as follows:

C: During the course of the 6 month production test the AEWM did very well in calling a crack - C. Thus, we keep the model for C as it was.

I: When the Plate No. 2 data was analyzed with this new model, the number of crack indications from the delayed crack areas was raised from 2 to 6. An analysis of the raw data shows the AE activity from delayed cracks consisted of high energy (100-4000 ringdown counts) and low minimum rate (3 events per 3 seconds).

L: The production tests showed that lack of fusion has infrequent occurrence (3) during 6 months of testing, and is not considered for repair. Thus, the L model is changed as shown, to monitor precursive activity for delayed cracking per previous discussion.

P: During the course of the 6 month production test, 3 rejectable porosity areas were detected by x-ray. Production AE monitoring detected 1 of the 3 repairs. AE data was recorded from only one of the two welds with missed porosity. Subsequent laboratory analysis of this recorded data detected the missed porosity using high energy ringdown counts. This new model for P opened the upper part of the energy window in hopes of improving on-line detection of rejectable porosity.

U: The U classification remains unchanged: all U indications have been confirmed as acceptable scattered porosity and have produced acceptable sizing measurement.

6.3 Production Study

A new production test was performed to evaluate the AEWM with the new flaw detection algorithm. Follow-up ultrasonic and penetrant testing was used to confirm flaws and correlate AE results after post-weld monitoring. X-ray inspection could not be performed on these hulls due to production scheduling.

Table 6.5 provides the delayed crack flaw detection data for the 4 hulls monitored with the new algorithm. The long outside weld on each hull was 100 percent real-time monitored, including the hand-welded root pass, and post-weld monitored. The length of the post-weld monitoring was determined by Production scheduling.

Table 6.6 summarizes the results. Key items presented are post-weld monitoring time, AE indications (with the new algorithm), and ultrasonic confirmation. The following paragraphs discuss the results.

Hull No. 1965 did have 2 delayed crack interpass indications (at 64 in. and 132 in.), which occurred about 2 minutes after the end of the weld pass Additional AE crack indications were recorded at 2-1/2 hours and 2-3/4 hours. Post-weld monitoring ended at 3 hours. 3 real-time indications occurred in Weld Pass 1. Follow-up UT inspection confirmed four of the crack indications.* The AEWM operator observed low level, high rate activity on the LED display just prior to the interpass delayed crack indications.

Post-weld monitoring of Hull No. 1979 gave 3 delayed crack indications in the area of interest (nose slope weld), after about 2 hours of post-weld monitoring. It was noted that after Weld Pass 8 and continuing thru Pass 10,there was a fair amount of low energy , high rate activity coming from the weld. There was 1 real-time AE crack indication during Weld Pass 3,and 3 real-time AE indications during Weld Pass 5. All 7 (3 delayed and 4 real-time) were confirmed by follow-up UT inspection.

In Hull No. 1994, 1 interpass delayed crack and 1 real-time flaw (porosity) were recorded, and both were verified by subsequent UT inspection. No precursive activity was noted by the AEWM operator.

Hull No. 2008 did have 1 delayed crack indication (132 in.) and 1 real-time indication (64 in.). It is interesting to note the real-time indication occurred in the root pass, and it reactivated in Weld Pass Numbers 2, 3, 6, and 8. After about 2-3/4 hours of post-weld monitoring, additional flaw-related activity occurred at the same location (64 in.) Both of these cracks (64 in and 132 in.) were later confirmed with ultrasonic inspection.

6.4 Discussion

Preliminary indications from a brief series of weld monitoring experiments performed in the LATP MM&T Weld Lab show encouraging delayed crack/precursor detection capabilities of the AEWM: a series of highly restrained butt welds were fabricated of 1.5 inch thick armor plate,

* confirmation of the fifth crack with UT inspection was inconclusive.

Table 6.5 DELAYED CRACK DETECTION DATA (Production)

HULL NO.	AE INDICATIONS	FLAW	CONFIRMATION	DISPOSITION	REMARKS
H-1965	LOW (Real-Time):				
	WP1 I40 (50")	Crack (TV) 50"	UT		No X-Ray Possible
	C2 (74")	Crack (TV) 74"	UT		
	I42 (114")	Crack 114"-116"	UT		
	I42 (116")				
	I36 (114")				
	Inter-Pass(Delayed):				
	WP6 I12 (64")	UT Inconclusive			All Indica. after welding stopped
	I18 (132")	Crack (TV) 132"			
	I1 (64")				
	I6 (64")				
	I1 (64")				
	End PWM				∿ 2½ hr.
H-1979	LOW (Real-Time):				
	WP3 I42 (130")	Crack (TV) 130"	UT		No X-Ray Possible
	WP5 I2 (82")	Crack (TV) 80"	UT		
	I1 (98")	Crack (TV) 99"	UT		
	C1 (128")	Crack (TV) 128"	UT		
	PWM				
	I3-17(7) (22")	Complex UT Return Signals 20" to 24"	UT		∿ 2 hr.
	P4 (20"				∿ 2 hr.
	P4 (3) (22")				∿ 2 hr.
	P4 (24")				∿ 2 hr.
	I7 (22")				∿ 2 hr.
	I4 (22")				∿ 2½ hr.
	I34 (22")				∿ 2½ hr.
	End PWM				∿ 3 hr.

Li = Linear
Lo = Local
TV = Transverse Crack
WP = Weld Pass
LOW = Long Outside Weld
LIW = Long Inside Weld

C = Crack
I = Incomplete Penetration
L = Lack of Fusion
RP = Root Pass
SOW = Short Outside Weld

P = Porosity
U = Unclassified
* = Suspected Delayed Cracking
PWM = Post-Weld Monitoring

Table 6.5 DELAYED CRACK DETECTION DATA (Production) continued

HULL NO.	AE INDICATIONS	FLAW	CONFIRMATION	DISPOSITION	REMARKS
H-1994	LOW (Real-Time):				
	WP2 P19 (4) (128")	5" Porosity(129")	UT		No X-Ray Possible
	Inter-Pass (Delayed)				
	P19 (126")				Reactivation
	I26 (114")	Crack (TV) 112"	UT		
	LOW (Real-Time):				
	WP3 I25 (132")				Reactivation
	End PWM				∿ 2½ hr.
H-2008	LOW (Real-Time):				
	RP C4 (64")	Crack (TV) 64"	UT		
	WP2 I115 (5) (64")				
	WP3 I28 (2) (64") C1 (64")				
	WP6 I9 (64")				
	WP8 U4 (64") C1 (64") I1 (64")				
	PWM				
	I9 (3) (132")	Crack (TV) 131"	UR		∿ 1½ hr.
	I9 (64")				∿ 3 hr.
	End PWM				∿ 3½ hr.

Li = Linear
Lo = Local
TV = Transverse Crack
WP = Weld Pass
LOW = Long Outside Weld
LIW = Long Inside Weld

C = Crack
I = Incomplete Penetration
L = Lack of Fusion
RP = Root Pass
SOW = Short Outside Weld

P = Porosity
U = Unclassified
* = Suspected Delayed Cracking
PWM = Post-Weld Monitoring

Table 6.6 PRODUCTION AE DETECTION OF TRANSVERSE CRACKS

HULL NO.	POST-WELD MONITORING TIME (hrs)	AE INDICATIONS				CONFIRMED FLAWS
		REAL-TIME	PRECURSOR	DELAYED		
				IP	PW	
H-1965	2.5	3	Yes[1]	2 @ 2 min	0	5[2]
H-1979	3	4	Yes	0	3 @ 2-3 hr.	7
H-1994	2.5	1	No	1 @ 2 min	0	2
H-2008	3.5	1[3]	Yes	0	2[3] @ 1.5-3 hr.	2

1. Yes/No means LED, not model.
2. 1 of 5 was "marginal" confirmation.
3. 1 Post-weld indication from same location as Real-Time indication.

IP = Interpass Monitoring
PW = Post-Weld Monitoring

with and without shield gas intentionally contaminated with hydrogen. In addition to considerable flaw-related AE activity during and immediately after the contaminated welding, delayed cracks were detected, located and characterized by the AEWM for up to 5 hours after welding. These delayed cracks were later confirmed radiographically and or ultrasonically. Large amounts of low energy, high rate AE were also detected during weld and post-weld monitoring in areas where delayed cracks occurred. In post-weld analysis of disk-recorded data, the high rate, low level AE activity was isolated to the location of the subsequently detected delayed cracks, both before and during the crack activity. Similar low energy, high rate AE activity was in evidence on the AEWM's analog module LED indicators during post-weld monitoring period on production welds that produced crack activity for up to about 12 hours after welding.

The new lab-based L model for detection of the precursive activity of delayed cracking did not work well in production (i.e., laboratory and production didn't seem to agree). The lab model for L (7:1, 16-80, 211, 0) appeared to have the rate test (7:1) set too high. Subsequent analysis of the disk-recorded data showed that the production monitoring AE model should be optimized as L = 4:1, 16-80, 211, 1. Figure 6.6 shows the results of analysis of the production recorded data with the L model a rate test at 4:1 and a locational tolerance of 1. The printouts show the presence of low level, high rate AE activity (at 64 inches from Sensor 1) precursive to delayed cracking: in Pass 1, low level AE activity is detected; in Pass 2, additional low level activity is present, then delayed crack indications (I) occur. We also see this in 3 additional weld passes and during post-weld monitoring.

The new I model (3:3, 96-4080, 242, 0) for detection of delayed cracks appears to be working well. On the four welds monitored with the new I model, 8 delayed crack indications (3 interpass and 5 post-weld) were located and characterized by the AEWM. Of the 5 post-weld indications, 3 were detected during post-weld pass interpass monitoring, and 2 were detected during monitoring after the weld was completed. Seven of these delayed crack indications were confirmed by follow-up ultrasonic inspection. One of the eight had "marginal" confirmation with ultrasonic inspection.

As discussed in Section 4.3.3, the AEWM provides intensity data to correlate with flaw severity. The original production line data showed crack severity numbers independent of crack size. The delayed crack studies support the theory that this is due to the ringdown count (RDC) window (96-1008) used in the initial production monitoring algorithm, and that raising the top of the energy window (i.e., 96-4080) will

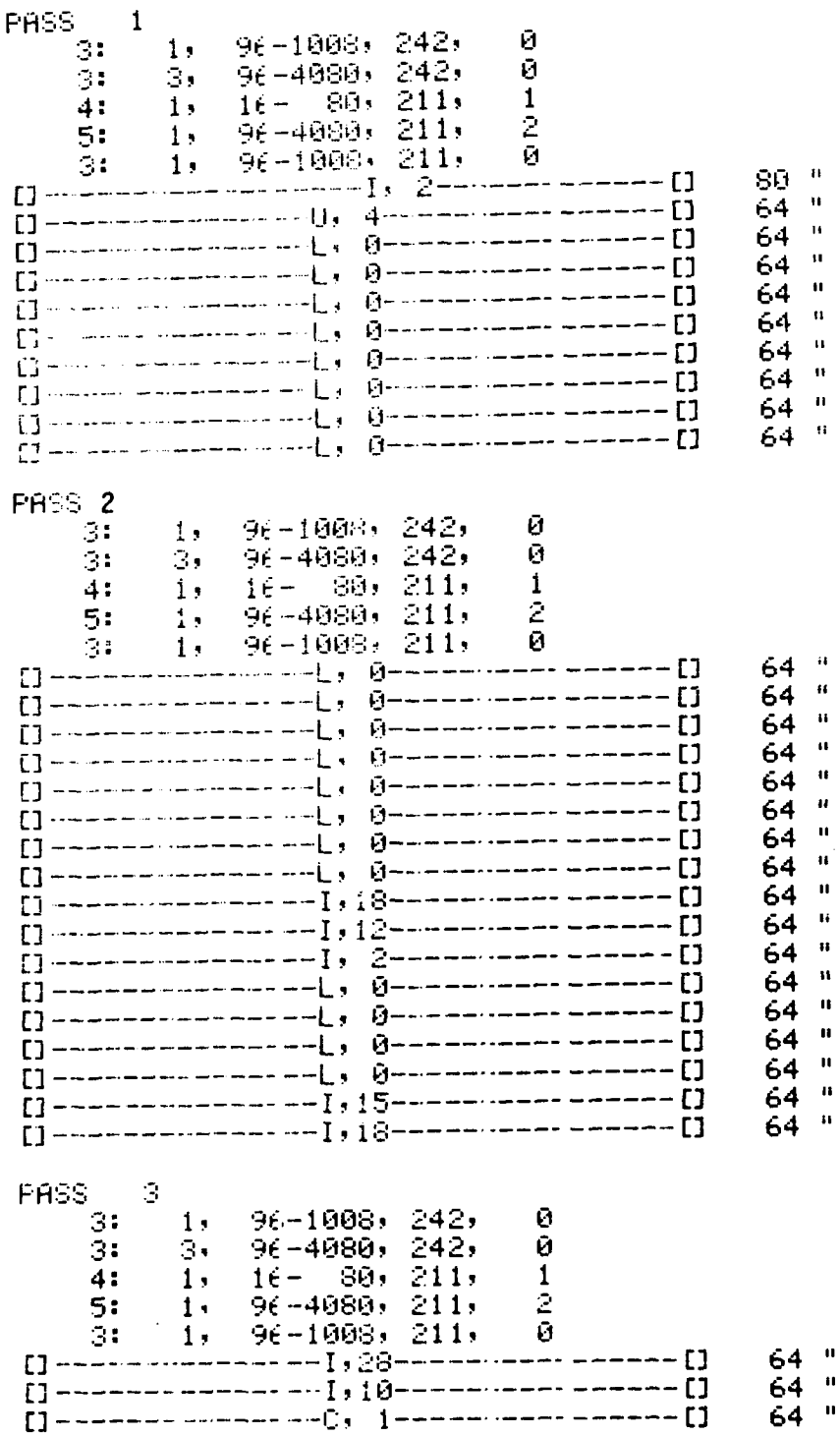

Figure 6.6 AE PRINTOUTS FOR HULL 2008 SHOWING LOW ENERGY HIGH RATE ACTIVITY IN AREA PRODUCING DELAYED CRACK

```
PASS   6
     3:    1,  9E-1008, 242,   0
     3:    3,  9E-4080, 242,   0
     4:    1,  1E-  80, 211,   1
     5:    1,  9E-4080, 211,   2
     3:    1,  9E-1008, 211,   0
[]----------------U, 4----------------[]    64 "
[]----------------C, 1----------------[]    64 "
[]----------------L, 0----------------[]    64 "
[]----------------L, 0----------------[]    64 "
[]----------------L, 0----------------[]    64 "
[]----------------L, 0----------------[]    64 "
[]----------------I, 1----------------[]    64 "

PASS   8
     3:    1,  9E-1008, 242,   0
     3:    3,  9E-4080, 242,   0
     4:    1,  1E-  80, 211,   1
     5:    1,  9E-4080, 211,   2
     3:    1,  9E-1008, 211,   0
[]----------------L, 0----------------[]    64 "
[]----------------L, 0----------------[]    64 "
[]----------------L, 0----------------[]    64 "
[]----------------L, 0----------------[]    64 "

 PWM
PASS  11
     3:    1,  9E-1008, 242,   0
     3:    3,  9E-4080, 242,   0
     4:    1,  1E-  80, 211,   1
     5:    1,  9E-4080, 211,   2
     3:    1,  9E-1008, 211,   0
[]-------------------------------I,20-[]   132 "
[]-------------------------------I, 9-[]   132 "

 PWM
PASS  12
DIS PASS 12
PASS  12
     3:    1,  9E-1008, 242,   0
     3:    3,  9E-4080, 242,   0
     4:    1,  1E-  80, 211,   1
     5:    1,  9E-4080, 211,   2
     3:    1,  9E-1008, 211,   0
[]-------------------------------I,11-[]   132 "
[]----------------L, 0----------------[]    64 "
[]----------------L, 0----------------[]    64 "
[]----------------L, 0----------------[]    64 "
[]----------------L, 0----------------[]    64 "
[]----------------I, 1----------------[]    64 "
```

Figure 6.6 (continued)

allow the intensity number to provide a better indication of crack size: the production data with the new model showed that the average RDC for I during welding was 3000, while the average RDC for I in post-weld monitoring was 1800. The top end RDC window (1080) used in the production, monitoring model would not allow such cracks to be sized. The new models ability to size flaws is not addressed in this effort since, no follow-up radiography could be performed due to production scheduling requirements.

Two porosity areas were detected by the AEWM with the new P model (P= 5:1, 96-4080, 211, 2). Ultrasonic inspection of these areas showed the complex UT return signals expected from clustered porosities.

7.0 TURRET RING REPAIR

A test that shows the effectiveness of using the AEWM for weld repair is described in this section. It is a turret ring weld repair, monitored with the AEWM, performed after two previous attempts to repair this weld had failed. Both times the repaired weld cracked, with the cracks revealed by subsequent radiographic inspection.

The third removal of the cracked weld area (by air-arcing) was monitored with the AEWM. During weld removal, reactivating crack indications were detected by the Weld Monitor, as shown in Figure 7.1. The welder continued air-arcing until the AEWM showed no evidence of AE crack noise. The printout in Figure 7.2 shows this result.

Repair welding was started and no further acoustic indications were observed until the repair was about two-thirds complete. Severe acoustic indications (see Figure 7.3) commenced at this point and persisted for several passes. Upon completion of the weld pass, the site was visually inspected and the crack could not be seen. Magnetic particle inspection was performed. The presence of a crack was still not verified. However, the welder air-arced out the new weld until the AEWM gave no more evidence of crack noise. He reported having seen a flaw in the weld during the arcing process.

Welding was resumed with no further rejectable acoustic emission indications (an I2 and I1 did occur). Figure 7.4 shows the results of the weld repair completion and the I1 indication. As determined in Section 5, such I indications are not considered serious.

Follow-up radiographic inspection revealed no rejectable defects in the repaired weld.

In conclusion, AE monitoring can allow a significant change in repair procedures. The AEWM can determine if a crack has been removed during the repair process: if flaw removal is successful, AE will show no further activity from the flawed area. It can detect weld defects during repair re-welding. Instead of waiting until the weld is completed and x-rayed, further repair can be accomplished on the spot, during the normal re-welding process.

OPERATION : RECORDING
PASS 3

F L NUMBER 1066 DATE 8/17/82

GAIN SETTINGS_____ WELD POSITION RING 4HR ARC

ACTIVE MODELS (C,I,L,P,U): (INITIAL FLAW CUT-OUT)

```
3:   1,  96-1008, 242,   0
3:   1,  96-1008, 242,   0
3:   1,  96-1008, 282,   0
5:   1,  96-1008, 211,   2
3:   1,  96-1008, 211,   0
```

REMARKS:

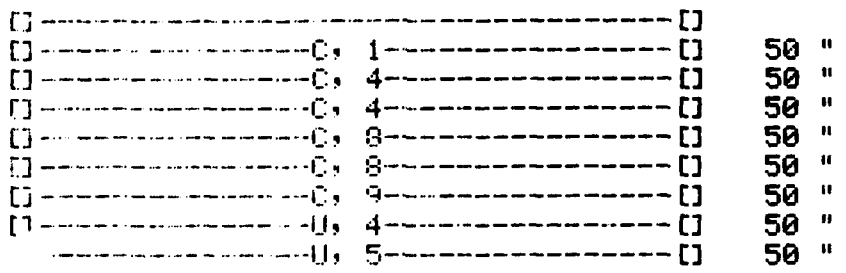

Figure 7.1 AE PRINTOUTS FOR TURRET RING REPAIR SHOWING INITIAL FLAW CUTOUT

OPERATION : RECORDING
PASS 6

HULL NUMBER ___1066___ DATE 2/12/82

GAIN SETTINGS_____ WELD POSITION__RING__

ACTIVE MODELS (C,I,L,P,U): AIR-ARC (INITIAL FLAW CUTOUT)

```
    3:   1,  96-1008, 242,   0
    3:   1,  96-1008, 242,   0
    3:   1,  96-1008, 282,   0
    5:   1,  96-1008, 211,   2
    3:   1,  96-1008, 211,   0
```

REMARKS:

[]----------[]

Figure 7.2 AE PRINTOUT FOR TURRET RING AIR-ARC CLEANED WELD

OPERATION : RECORDING
PASS 11

HULL NUMBER ___1066___ DATE _8_/_17_/_83_____

GAIN SETTINGS_____ WELD POSITION__RING REPAIR___

ACTIVE MODELS (C,I,L,P,U):

```
    3:    1,  96-1008, 242,   0
    3:    1,  96-1008, 242,   0
    3:    1,  96-1008, 282,   0
    5:    1,  96-1008, 211,   2
    3:    1,  96-1008, 211,   0
```

REMARKS:

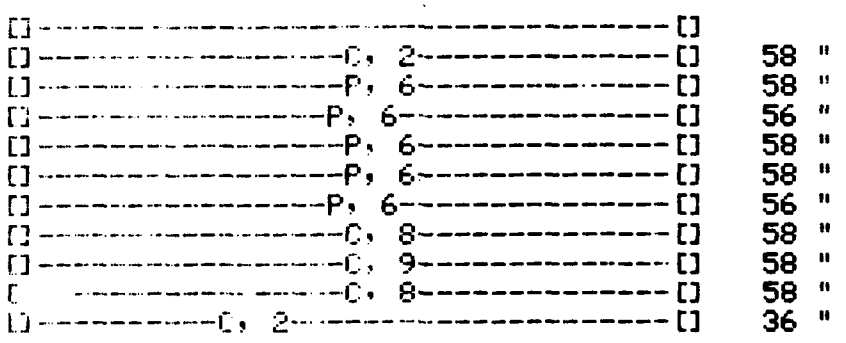

Figure 7.3 AE PRINTOUT FOR TURRET RING CRACK DURING REPAIR WELDING

OPERATION : DISPLAY 22
PASS 2

HI' '. NUMBER 1066 DATE 8/17/83

GAIN SETTINGS_____ WELD POSITION RING

REPAIR AFTER CUTTING FLAW OUT AGAIN

ACTIVE MODELS (C,I,L,P,U):

```
3:   1,  96-1008, 242,   0
3:   1,  96-1008, 242,   0
3:   1,  96-1008, 282,   0
5:   1,  96-1008, 211,   2
3:   1,  96-1008, 211,   0
```

REMARKS:

```
[]-------------------------------------[]
[]---------------I, 1----------------[]   50 "
```

Figure 7.4 AE PRINTOUT FOR TURRET RING FINAL WELD REPAIR

APPENDIX

GRINDING BLINDING STUDIES

GRINDING BLINDING

When mechanical grinding occurs on a hull during monitoring with the AEWM, it can produce a large acoustic signal which is acquired by the Monitor. The Monitor has provisions where this type of signal is ignored (i.e., it does not produce flaw indications). However, the Monitor is effectively "blinded" during the grinding period: it can miss flaws when loud grinding takes place.

This happened during 10 percent of the production monitoring on Phase II of this project. Thus, on this Phase III, GARD performed a) a spectral analysis on the grinding and chipping signals in an attempt to determine whether frequency discrimination can minimize the blinding problem, and b) a directional transducer evaluation to determine whether sensor directivity can minimize the blinding problem.

Neither was successful within the scope of effort available to this activity. Conclusion after the spectral analysis was that monitoring at higher frequencies (greater than 600 kHz) would have to be investigated. This would potentially involve system hardware and software rework, requiring extensive weld monitoring for new flaw algorithm development. The conclusion, after on-hull experimentation with the only commercially-available directional AE transducers known to GARD, was that they were not directional enough to help. Special transducer configurations would have to be tried. Again, this was beyond the scope of our planned activity in this area.

Attached are reports on both of the above subjects.

GARD, INC.

TO A1-63 Project File DATE December 2, 1982

FROM M. J. Zroka *M. J. Zroka*

SUBJECT Mechanical Blinding Noise Analysis

On our recent trip to Lima, recordings of two mechanical noise sources, chipping hammer and grinding, were acquired using the Honeywell 101 Recording System configured for wideband group II recording. Three transducer types and as many mounting techniques were utilized. The chipping hammer noise source was recorded at Station 3; the approximate area of application is indicated in Figure 1 as are the transducer locations used in the recordings. Grinding noise was acquired at Station 1 during a non-welding interval. The hull area in which the grinding was done and the various transducer locations used in acquiring the resultant noise are also indicated in Figure 1.

A block diagram of both the field data acquisition system and GARD laboratory data analysis system is shown in Figure 2 for reference. The recorded data were reproduced at slower tape speeds to accommodate the system's bandwidth - nominally 100 kHz. The low pass filter employed to prevent aliasing effectively limited the highest frequency in any analysis to a multiple of 100 kHz, the multiple being directly related to tape speed reduction. This is reflected in Table 1 which reveals various spectrum characteristics for several reproduce speeds.

Selected spectrum plots from which the data in Table 1 were obtained are included at the end of this memo for your files. The table indicates that chipping hammer noise spectrum levels are down 30dB from peak values from roughly 225 kHz and beyond. In addition, it reveals that the frequency at maximum amplitude varies with transducer type; the higher frequencies resulted from using the D/E 140 magnetic mount and AET-750 transducers. Peak frequency amplitudes are also shown to be transducer dependent. There is an approximate 20dB difference comparing the D/E 140 magnetic mount and AET-375 transducers with the D/E 140 waveguide mount and AET-750 transducers. These results clearly reflect transducer freq-quency response effects on the measured signals.

The grinding noise spectrums revealed a much broader range over which spectrum levels were within 30dB from peak values, typically out to 1 MHz (See Table 2). Peak values, and actually entire spectrum levels as well, were >10dB down from corresponding chipping hammer noise plots. This reflects the lower intensity characteristic of the grinding noise compared to that generated by the chipping hammer. Grinding noise spectrum levels were within 20dB of peak values out to, at the minimum, 150 kHz. Again, the D/E 140 magnetic mount transducer exhibited a higher frequency at maximum amplitude than the AET-375 owing to its 140 kHz resonant characteristic.

The data in Table 2 also reflect the high frequency attenuation characteristics of the hull. The transducer mounted on the same side that the grinding was done yielded spectrums whose amplitudes were within 20dB from peak values out to 250 kHz. Mounting the transducer on the opposite side (see Figure 1) reduced this range to 150 kHz, a difference of 100 kHz. It seems likely these latter results would have greater significance in determining additional AEWM signal processing requirements since grinding would never be expected to be carried on physically close to a simultaneous welding operation.

Since a welding operation was not monitored on this trip, the spectrum results generated for the noise sources recorded will have to be compared with spectrum characteristics of previously acquired weld operation induced noise, particularly within narrow bands centered around 110, 150, 200, and 270 kHz. These are the lowest four center frequencies utilized in the AEWM's comb filter. It is likely that the noise spectrum components within the lowest two bands, and to a lesser extent the next two, will mask out flaw induced AE spectrum components due to large differences between source intensities.

Time domain analysis included the generation of autocorrelation function coefficients for several sampled record lengths of each noise source. The resultant plots reveal the type of repetitive correlation peaks (plus and minus) associated with a time series comprised from a dominant narrow spectrum band. Several plots are included at the end of this memo for your inspection. The autocorrelation data would not be of any real analytical value (e.g., in a signal processing algorithm for flaw detection or classification) in meeting this particular application's objectives. Its sole usefulness, however, is in regards to identifying, or classifying, the signal processing problem at hand. The data tends to support a signal corrupted by noise model pitting a relatively small amplitude, transient, flaw AE signal against a higher amplitude, highly tonal, and continuous additive noise source. This model can be represented as shown in Figure 3.

The AEWM currently bases detection of a flaw-related event primarily on the ringdown counts generated by AE events occuring within a fixed time period. The AE signals are passed through a 100 kHz - 400 kHz bandpass filter before they are processed. A comb filter comprised of eight narrowband bandpass filters is used to acquire AE classification data. Filter center frequencies range from 110 kHz to 920 kHz.

Both, the chipping hammer and grinding noise, have sufficient amplitude after the 100 kHz input signal cut-off; and being continuous, they severely compromise the detection scheme. Extending the low frequency input signal cut-off to 250 kHz to eliminate these noise components from the AEWM is one approach to correct this condition. The problem with this, however, is that the useful signal components below 250 kHz are also eliminated. The

detection scheme used in the AEWM would have to be necessarily modified and then field-proven all over again. In addition, the lowest three comb filter center frequencies, 110 k, 150 kHz, and 200 kHz, would be effectively useless. Depending on how efficient the input filter is in passing signals only above 250 kHz, effects on the results derived from the 270 kHz bandpass filter, an important AE flaw classifier, will also have to be considered. Software modifications that require re-development of proven algorithms used in the AEWM would have to be carefully tested to ensure their validity.

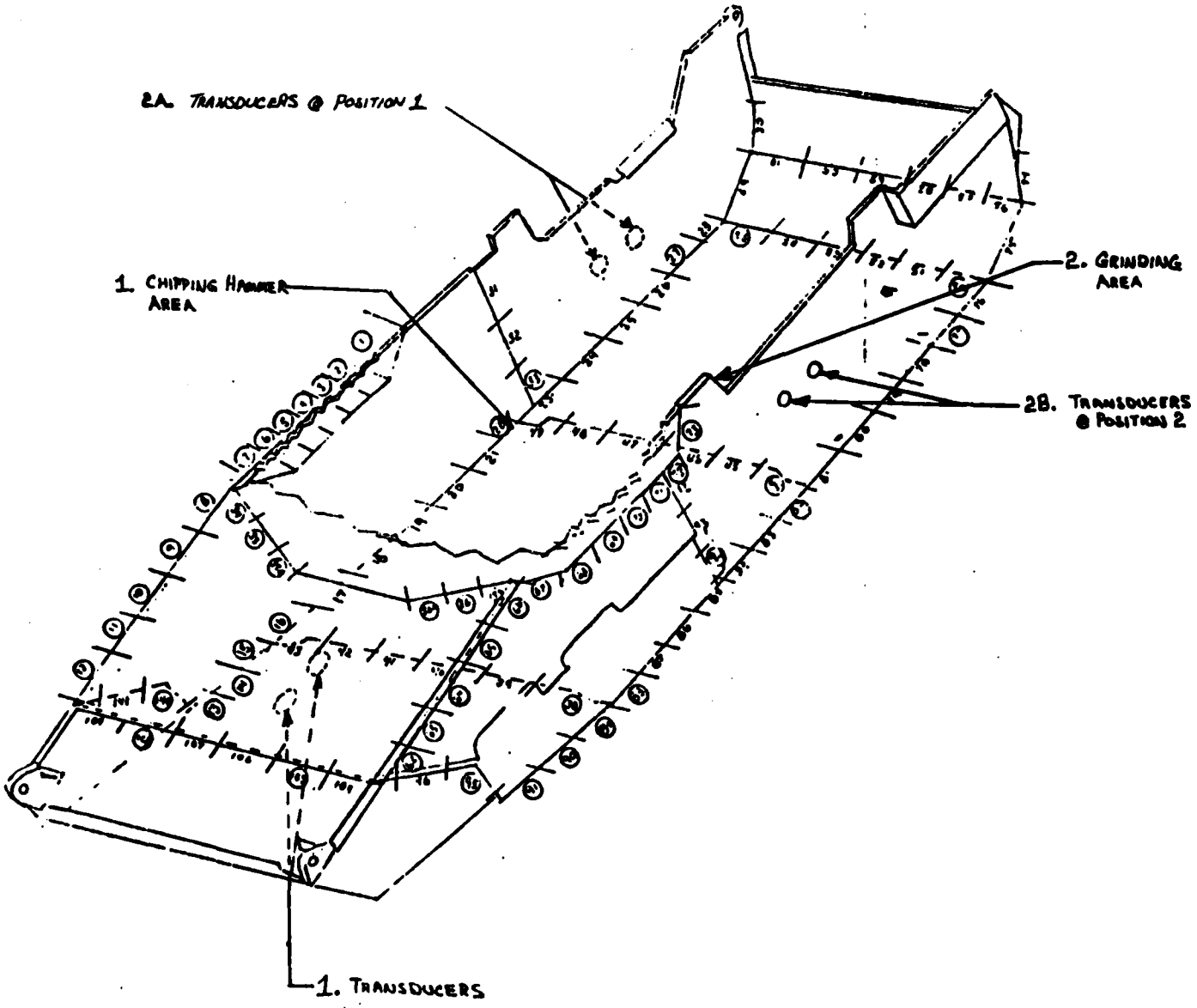

Figure 1 Transducer Placement and Noise Source Area Locations

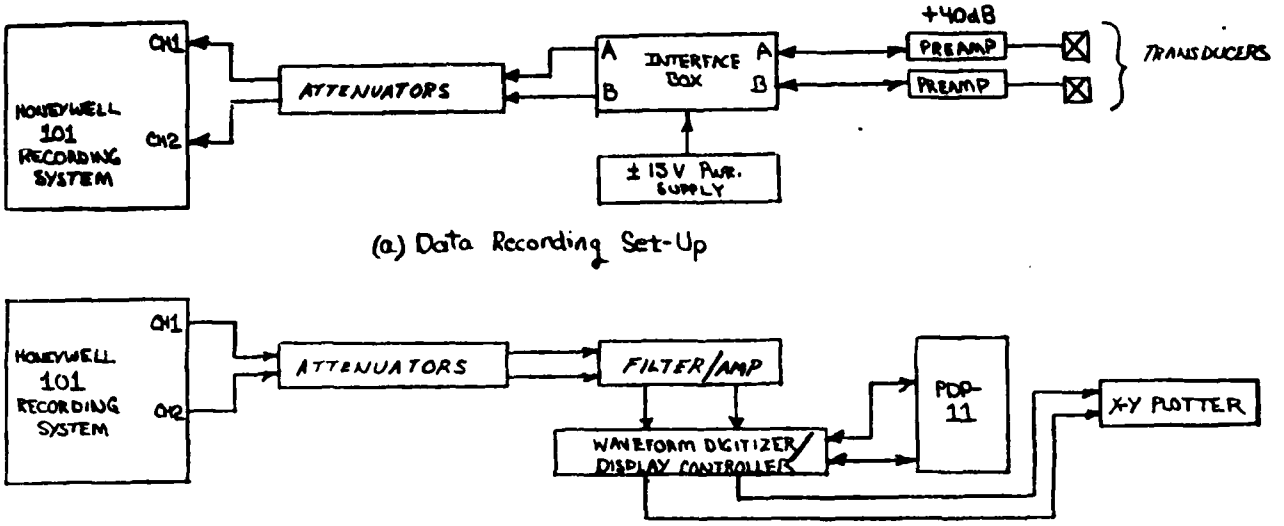

Figure 2 (a) Data Recording Set-Up
(b) Data Analysis Set-Up

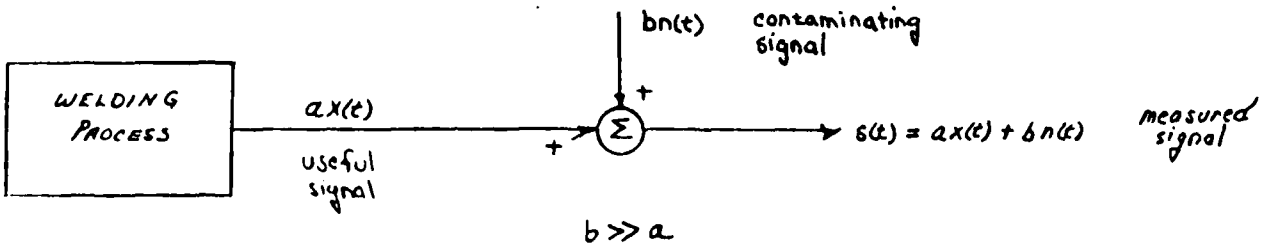

Figure 3 Measured Signal Model

SPECTRUM CHARACTERIZATION TABLE 1

CHIPPING HAMMER AE

ANALYSIS RANGE	LOW PASS FILTERING	TRANSDUCER	FREQ. AT MAX. AMP.	MAX. AMP. dBV^2/Hz	SPECTRUM WIDE WITHIN 30dB FROM PEAK
0 - 1.5MHz	800kHz	D/E 140 MAGNETIC	127.5 kHz	-88.75	0 - 225kHz
0 - 1.5MHz	800kHz	AET-375 (3048)	86.25kHz	-92.00	0 - 225kHz
0 - 1.5MHz	800kHz	AET-375 (3313)	101.25kHz	-88.50	0 - 285kHz
0 - 1.5MHz	800kHz	D/E 140 WAVEGUIDE	67.5kHz	-109.50	0 - 225kHz
0 - 1.5MHz	800kHz	AET-750	135 kHz	-105.00	0 - 210kHz
0 - 750kHz	400kHz	D/E 140 MAGNETIC	127.5kHz	-95.00	0 - 240kHz
		AET-375 (3048)	103.1kHz	-94.50	0 - 243.kHz
		AET-375 (3313)	86.25kHz	-94.50	0 - 303 kHz
		D/E 140 WAVEGUIDE	75kHz	-120.00	37.5 - 225 kHz
		AET-750	142.5kHz	-95.50	0 - 232.5 kHz
0 - 375 kHz	200 kHz	D/E 140 MAGNETIC	133.1kHz	-91.00	0 - 202.5kHz
		AET-375 (3048)	121.9kHz	-92.50	0 - 223.12 kHz
		AET-375 (3313)	91.88kHz	-93.00	0 - 176.8 kHz
		D/E 140 WAVEGUIDE	76.9kHz	-106.00	37.4 - 178.1kHz
		AET-750	140.6kHz	-110.00	0 - 206.25 kHz
0 - 750kHz	100-400kHz	D/E 140 MAGNETIC	112.5kHz	-100.00	48.8 - 243.8kHz
		AET-375 (3313)	86.25kHz	-98.50	56.2 - 375 kHz

GRINDING AE

TABLE 2

ANALYSIS RANGE	LOW PASS FILTERING	TRANSDUCER	FREQ. AT MAX. AMP.	MAX. AMP. dBV²/Hz	SPECTRUM RANGE WITHIN 30dB FROM PEAK	SPECTRUM RANGE WITHIN 20 dB FROM PEAK
0-1.5MHz	800 kHz	AET-375 (3048)	105kHz	-108.5	0-1.12 MHz	0-195kHz
		D/E 140 MAG. @ 1	120kHz	-101.0	0-975 kHz	0-142.5kHz
		D/E 140 MAG. @ 2	120kHz	-97.5	0-1.05 MHz	0-255 kHz
0-750kHz	400kHz	AET-375 (3048)	90 kHz	-109.5	0-438.8kHz	0-168.8kHz
		D/E 140 MAG. @ 1	127.5kHz	-99	0-401.2kHz	0-150kHz
		D/E 140 MAG. @ 2	120kHz	-106	0-345 kHz	0-244 kHz
0-375kHz	200kHz	AET-375 (3048)	91.9kHz	-107.0	0-215.6 kHz	0-135.6 kHz
		D/E 140 MAG @ 1	133.1kHz	-109.0	0-232.5 kHz	0-193.1kHz
		D/E 140 MAG @ 2	130.3kHz	-107.5	0-228 kHz	0-178 kHz

Power Spectrum Plots

Chipping Hammer Noise

Grinding Noise

Autocorrelation Plots

Chipping Hammer

AET-375 (3313)

CHIPPING HAMMER INVERTED NOISE SPECTRUM

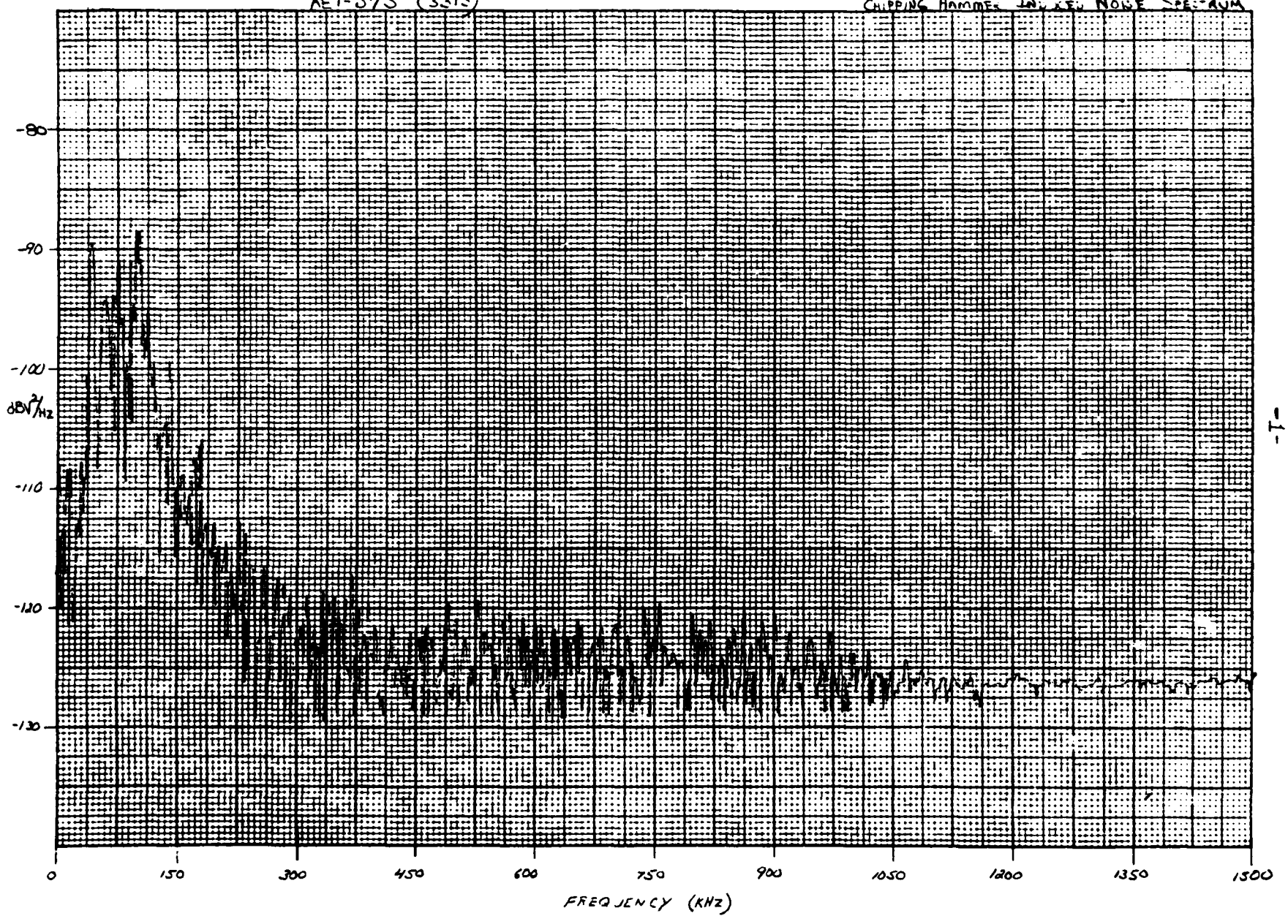

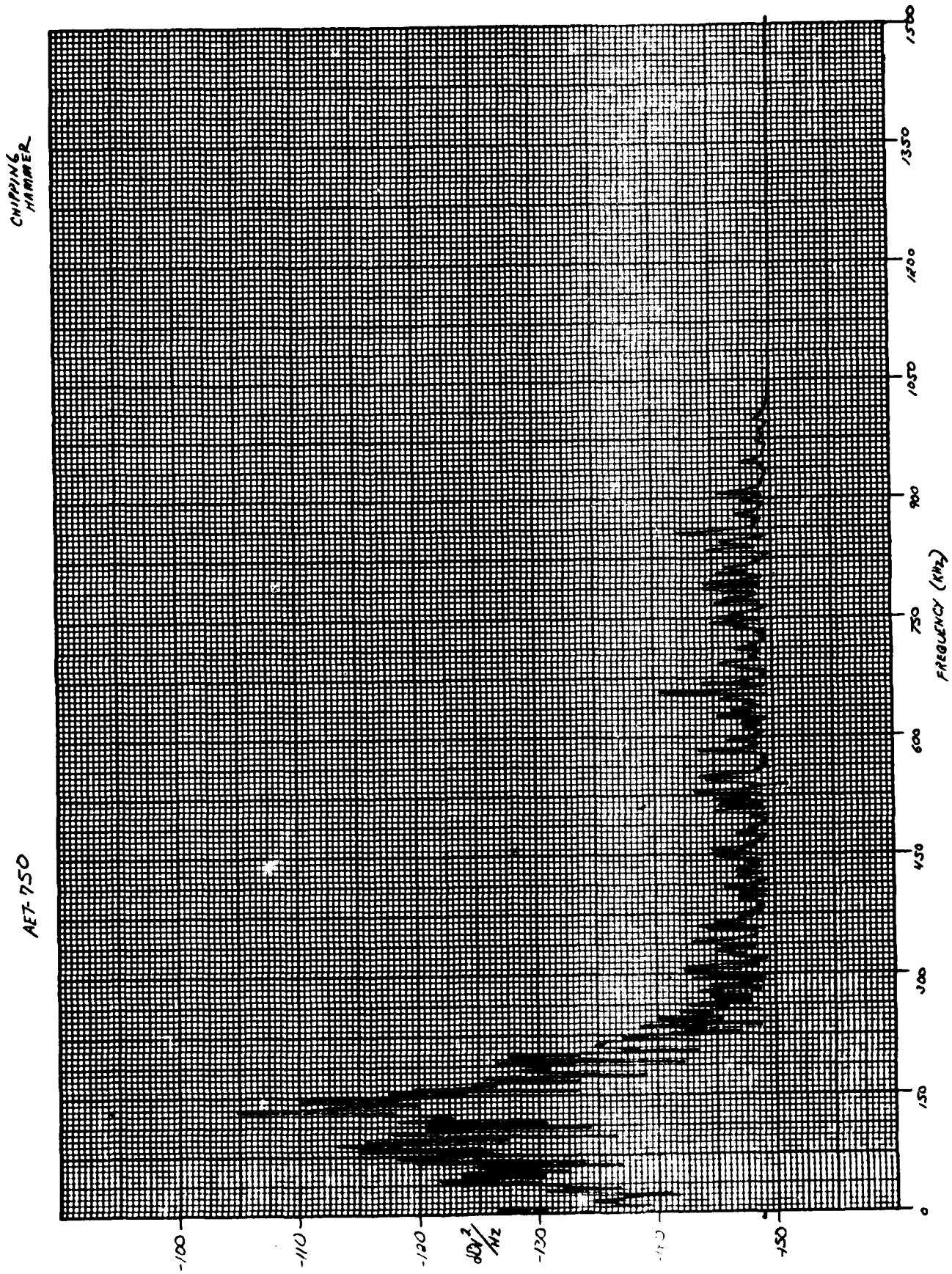
CHIPPING HAMMER
AET-750
-100
-110
-120
dBy²/Hz
-130
-140
-150
0
150
300
450
600
750
900
1050
1200
1350
1500
FREQUENCY (KHz)

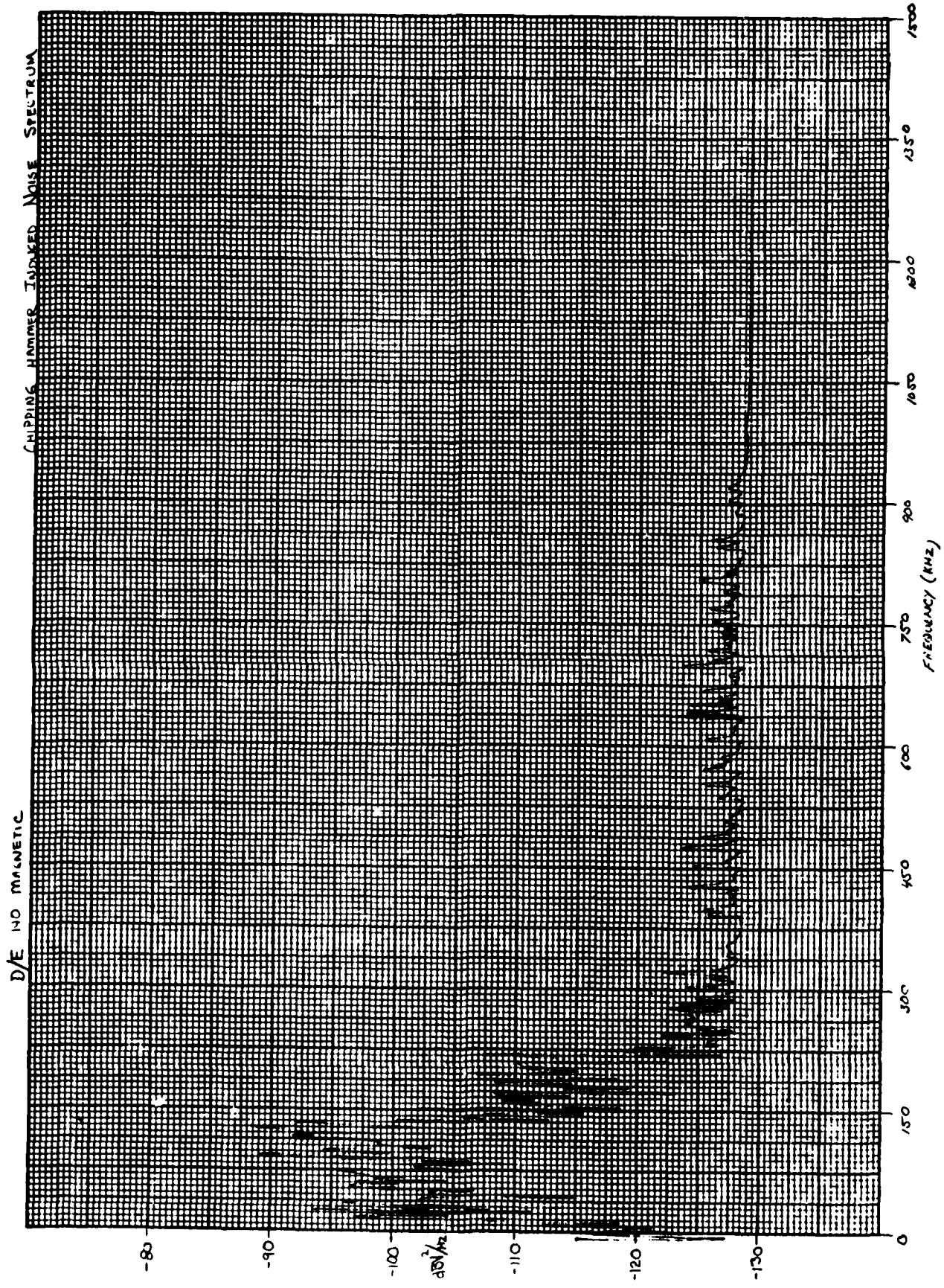
CHIPPING HAMMER INDUCED NOISE SPECTRUM
D/E NO MAGNETIC
-80
-90
-100
-110
-120
-130
dBV²/Hz
0
150
300
450
600
750
900
1050
1200
1350
1500
FREQUENCY (KHz)

SB 140 3M WAVEGUIDE

CHIPPING HAMMER

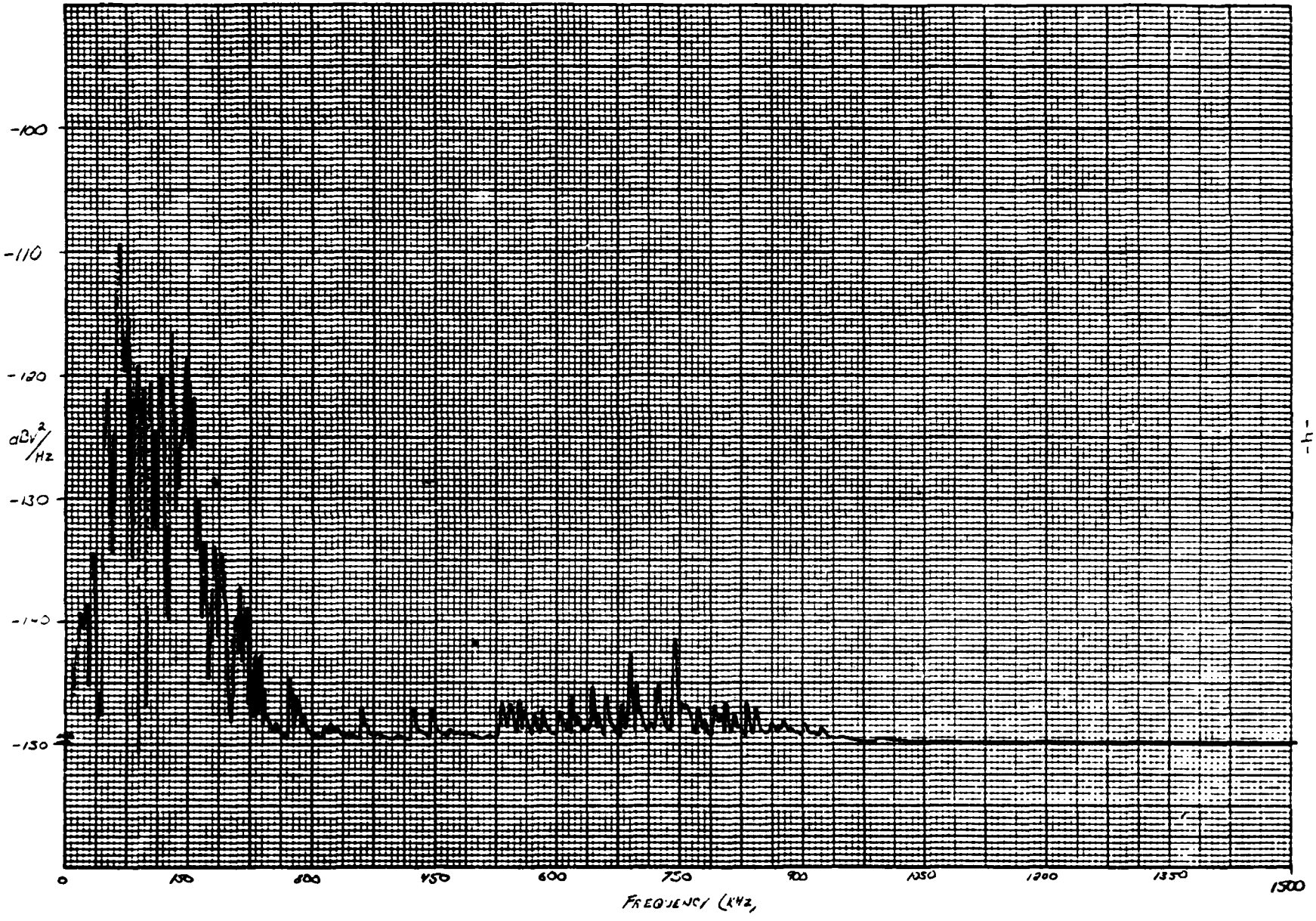

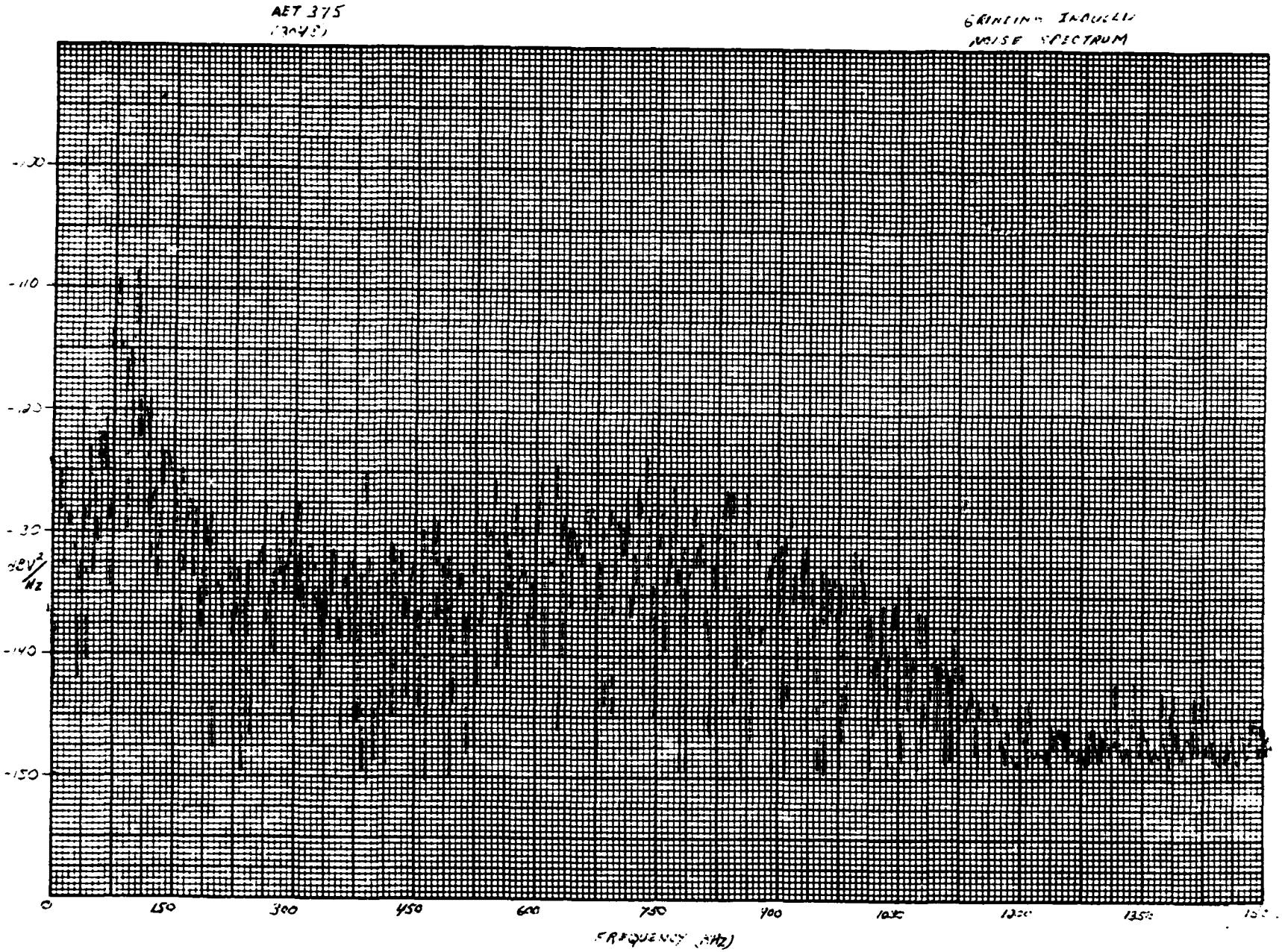
AET 375
GRINDING INBOARD
NOISE SPECTRUM
-100
-110
-120
-130
-140
-150
dBV²/Hz
0
150
300
450
600
750
900
1050
1200
1350
FREQUENCY (kHz)

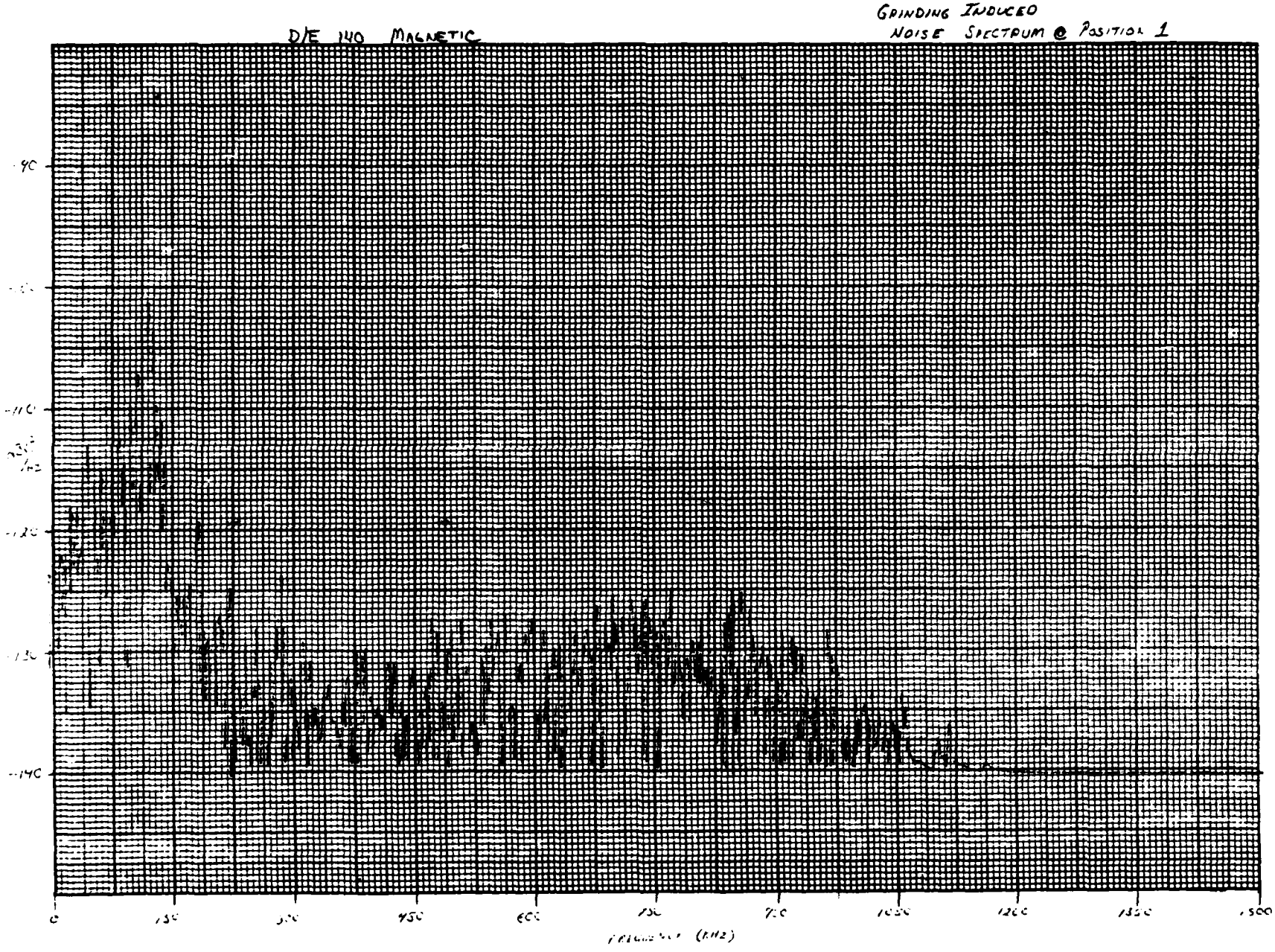
D/E 140 MAGNETIC
GRINDING INDUCED
NOISE SPECTRUM @ POSITION 1
-90
-110
-120
-130
-140
0
150
300
450
600
750
900
1050
1200
1350
1500
FREQUENCY (KHz)

D/E 140 MAGNETIC

GRINDING INDUCED
NOISE SPECTRUM @ POSITION 2

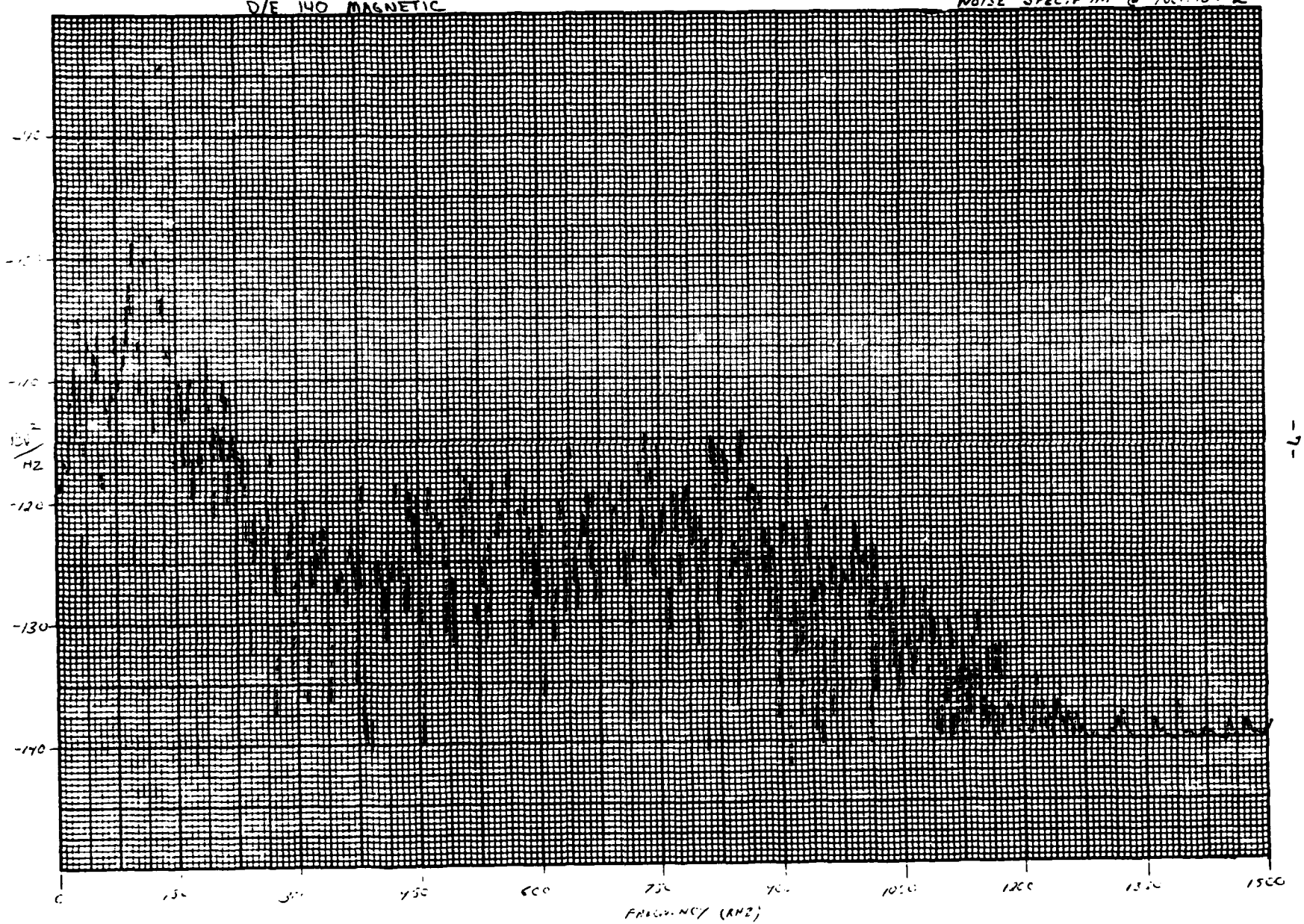

Autocorrelation Plot
Chipping Hammer AE
AET-375 (3313)
100kHz-400kHz BPF
2mHz Sampling

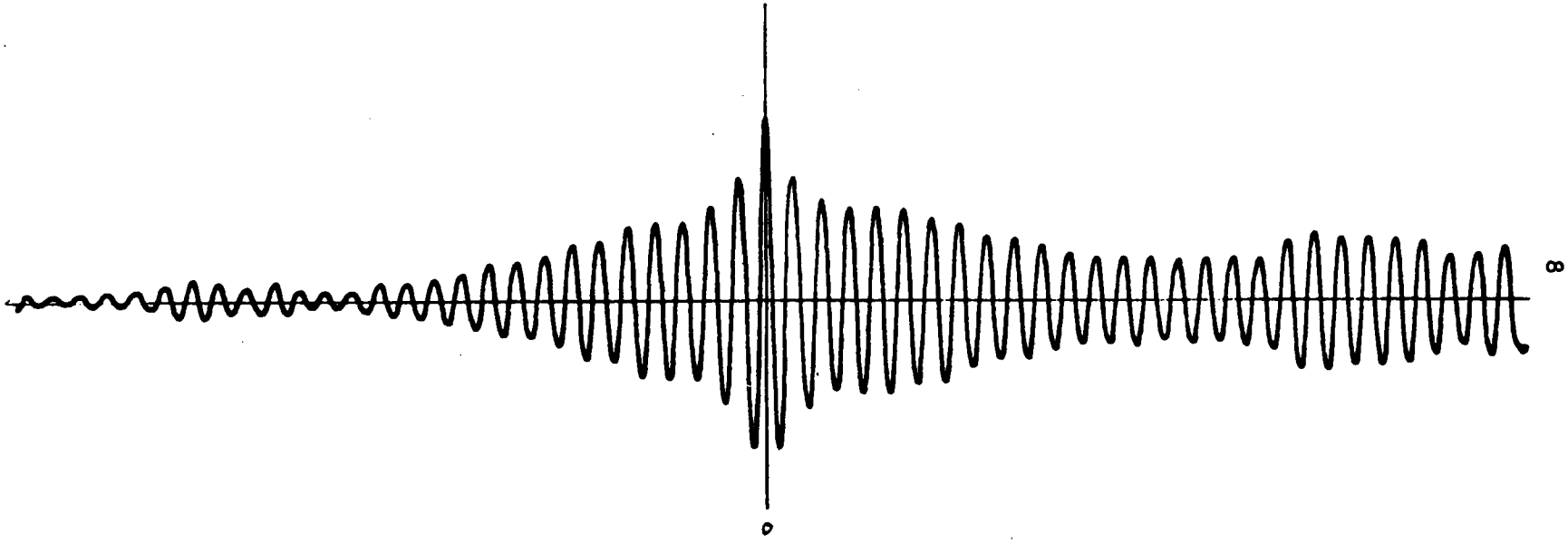

Autocorrelation Plot
Chipping Hammer AE
AET-375 (3313)
800 kHz LPF
3 mHz Sampling

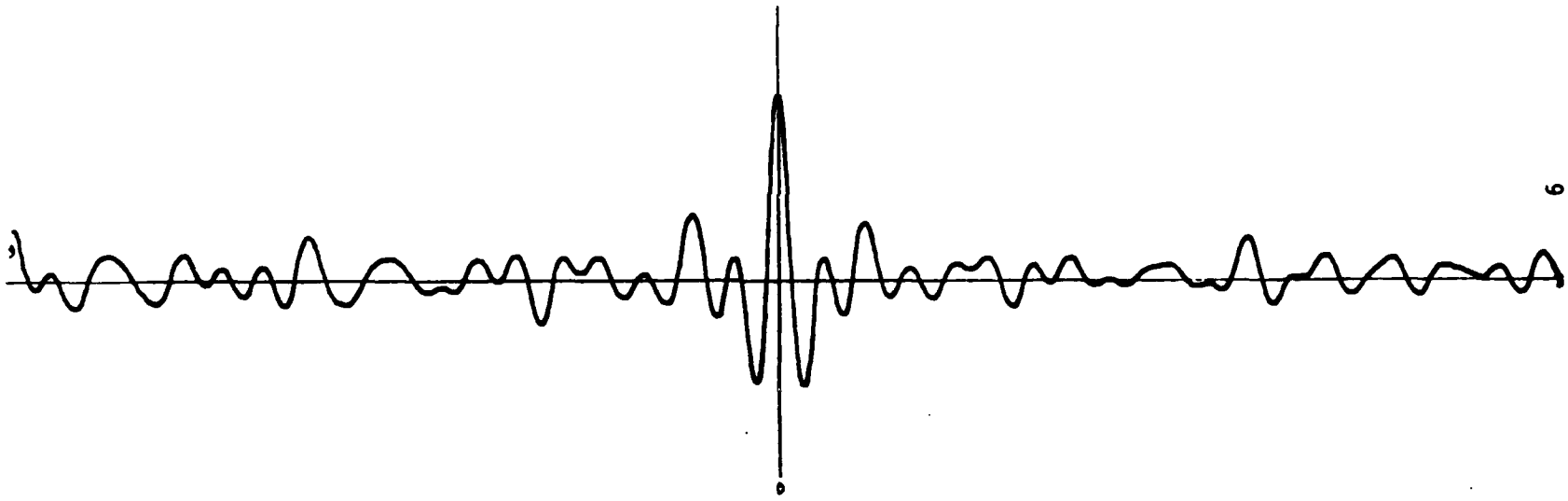

TO: A1-63 File Date: February 1983

FROM: I.R. KRASKA

SUBJECT: Directional Transducers

To aid in the attempt to reduce the effects of AEWM "blinding" from grinding and chipping hammer noise, we evaluated the use of newly developed directionally-sensitive transducers. Directional sensitivity tests were made with purchased Dunegan/Endevco D220M1 acoustic emission transducers. Laboratory tests were conducted on a large (3x5 foot) steel plate to minimize the effect of edge reflected signals on transducer response. A block diagram of the data acquisition system is shown in Figure A-1. The distance from the sensor to the acoustic emission source is 7 inches.

Peak amplitude response of the sensor to a acoustic emission signal was measured for several angles of orientation of the sensor to the source. The results of the experiment are shown in Figure A-2. The peak response of the sensor is indicated at the zero position on the polar plot. The results show that the transducer response is relatively flat in the forward-directed quadrant of the plot, dropping to only -4db at the band edges. Maximum signal rejection (-12db) occurred when the sensor was 200/160 degrees off to either side of the peak response position. A narrow lobe of higher sensitivity (-7db) was noticed at the 180 degree position.

Tests were also conducted on a M1 tank hull at LATP to determine the effects of hull geometry (see Figure A-3) on transducer response. The data acquisition system used for the hull experiment was the same arrangement used in the laboratory tests.

The results of the experiment showed peak sensor response in the forward direction. Maximum signal rejection (-5db) occurred when the acoustic emission signal source was located along the welds where simultaneous grinding might be expected during weld monitoring with the AEWM. This low signal rejection was not sufficient to overcome the acoustic grinding noise generated while simultaneously monitoring a weld for flaws.

Thus this approach was not pursued further.

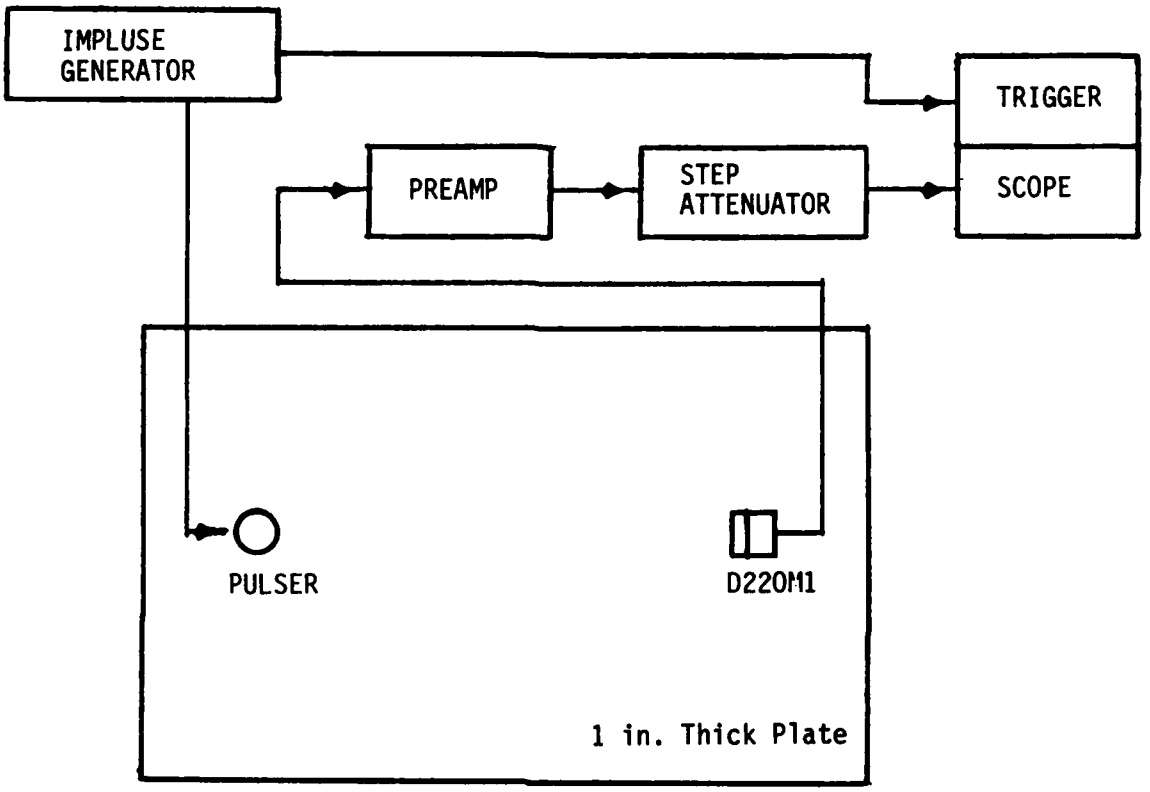

Figure A-1 TEST SET UP FOR DIRECTIONAL SENSITIVITY MEASUREMENT OF D220M1

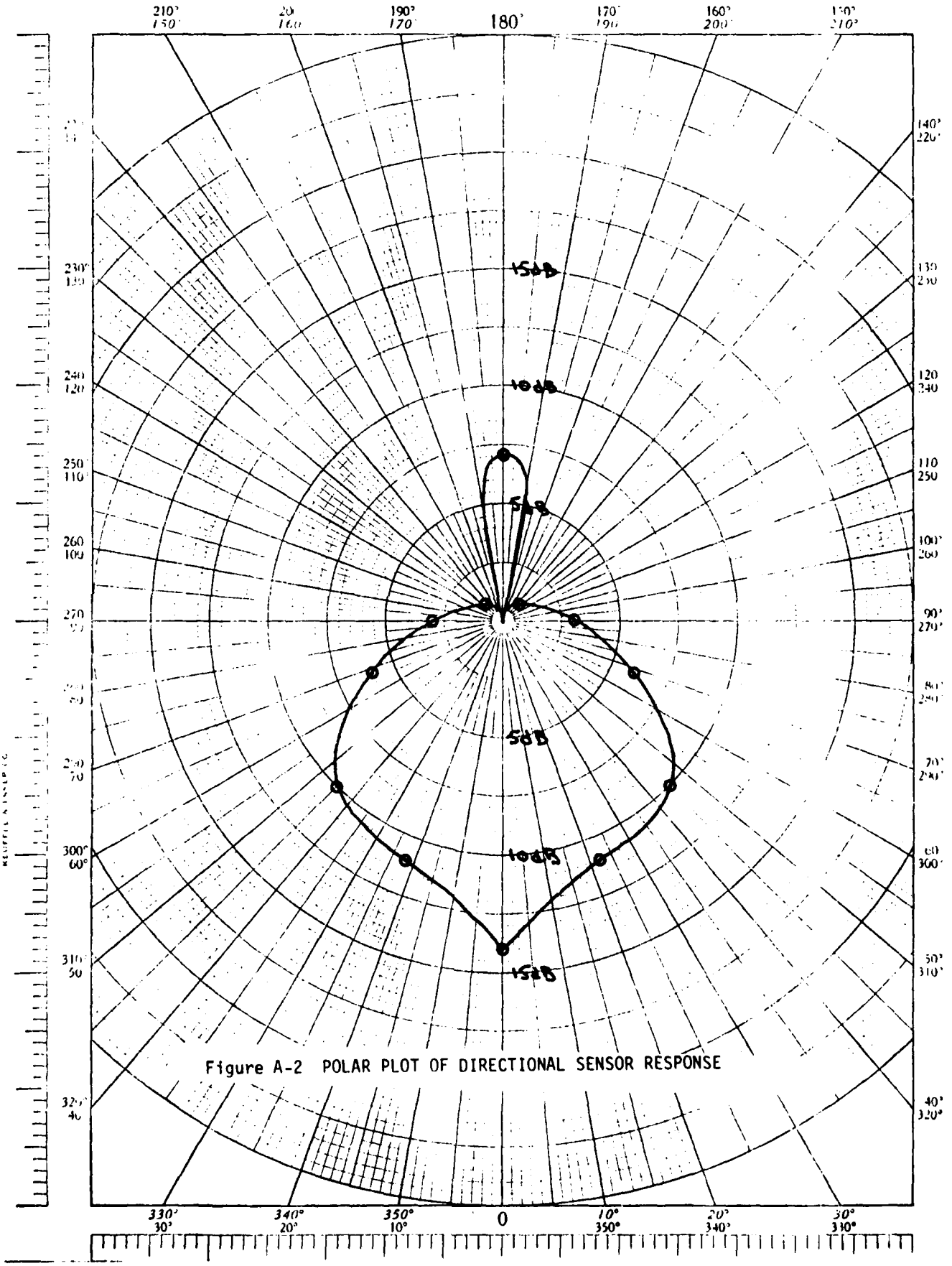

Figure A-2 POLAR PLOT OF DIRECTIONAL SENSOR RESPONSE

AD-A154 168 PRODUCTION VERIFICATION OF THE ACOUSTIC EMISSION WELD MONITOR(U) CHAMBERLAIN NATIONAL NILES IL GARD DIV I R KRASKA ET AL. MAY 84 TACOM-TR-12988 2/2

UNCLASSIFIED DAAE07-82-C-4116 F/G 11/6 NL

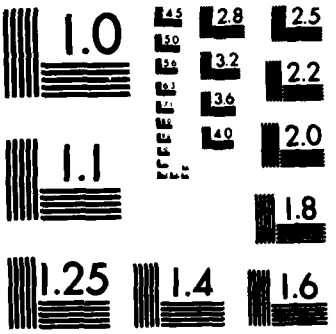

MICROCOPY RESOLUTION TEST CHART
NATIONAL BUREAU OF STANDARDS-1963-A

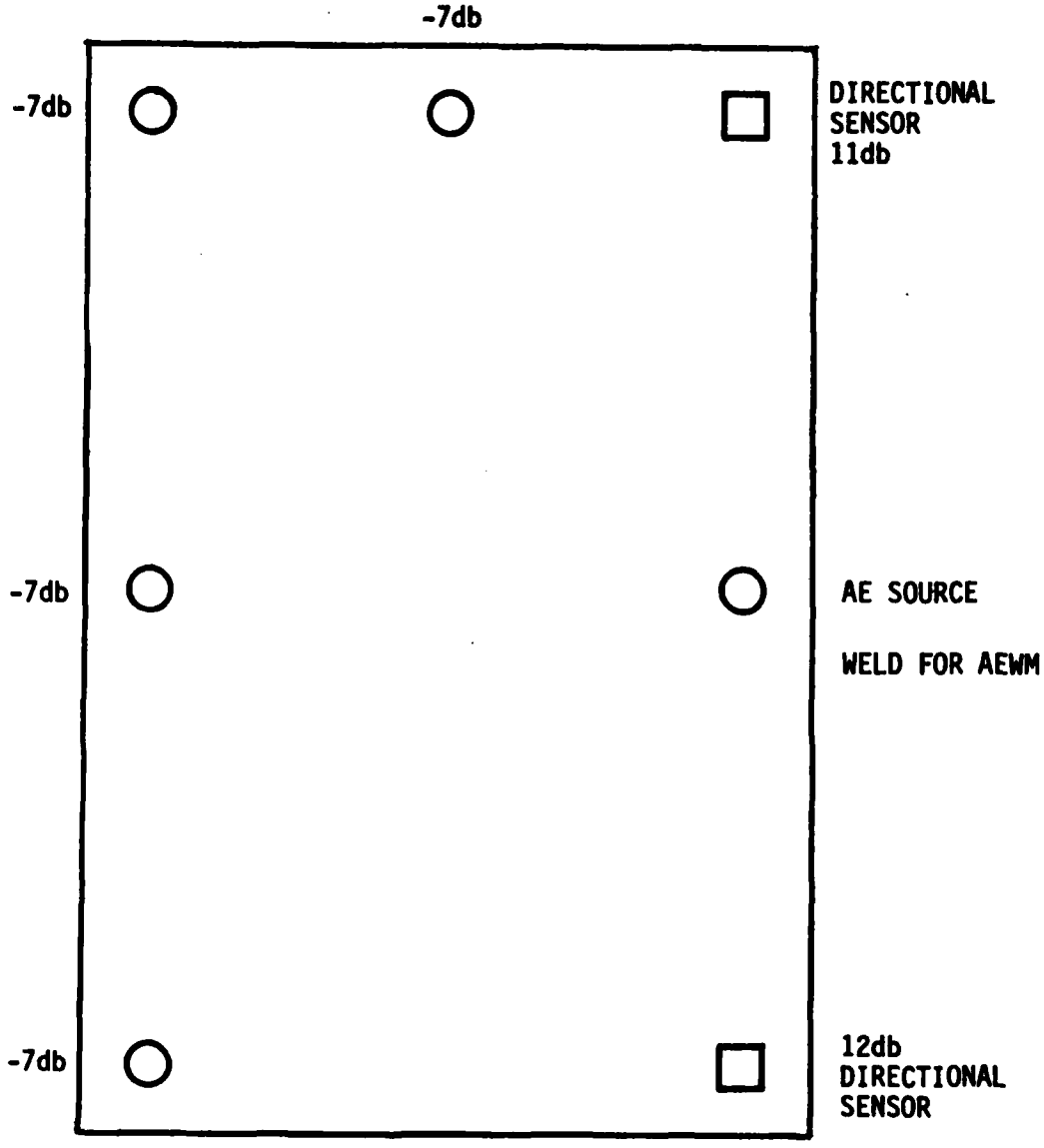

Figure A-3 DIRECTIONAL SENSOR RESPONSE ON M1 TANK HULL

END

FILMED

7-85

DTIC